Lattice determination of baryon-baryon potentials

Noriyoshi Ishii
RCNP, Osaka Univ.
for HAL QCD Coll.

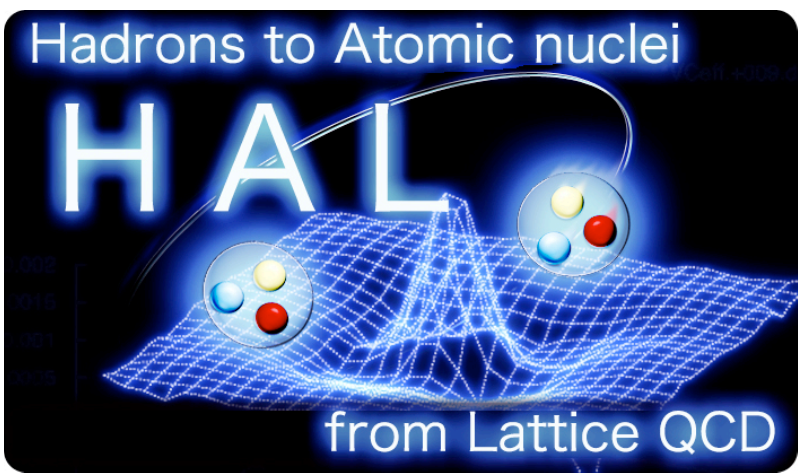

RCNP, Osaka Univ:	N.Ishii, K.Murano
Univ. Tsukuba:	H.Nemura, K.Sasaki,
Univ. Birjand:	F.Etminan
RIKEN:	T.Doi, T.Hatsuda, Y.Ikeda
Nihon Univ:	T.Inoue
YITP(Kyoto):	S.Aoki, T.Miyamoto,
	S.Gongyo, D.Kawai
Stony Brook Univ:	T.Iritani

Nuclear physics and Quantum Choromodynamics(QCD)

◆More than 40 years have been passed since the establishment of QCD

◆Meanwhile, nuclear physics and QCD have made independent progress.

◆Now, these two start to merge.

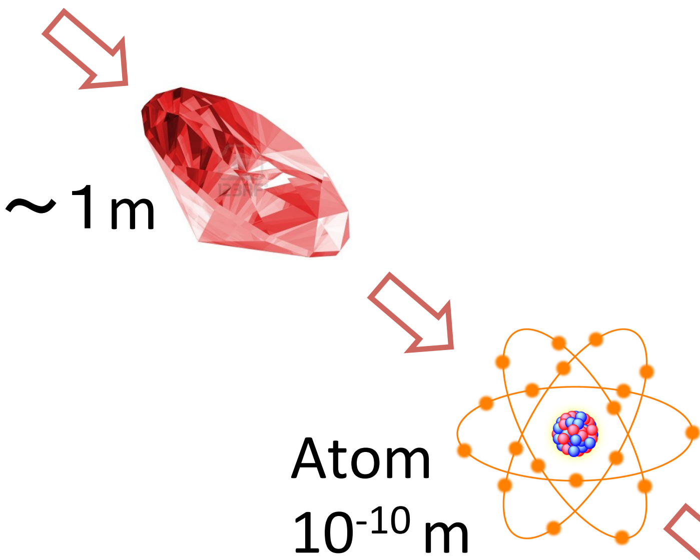

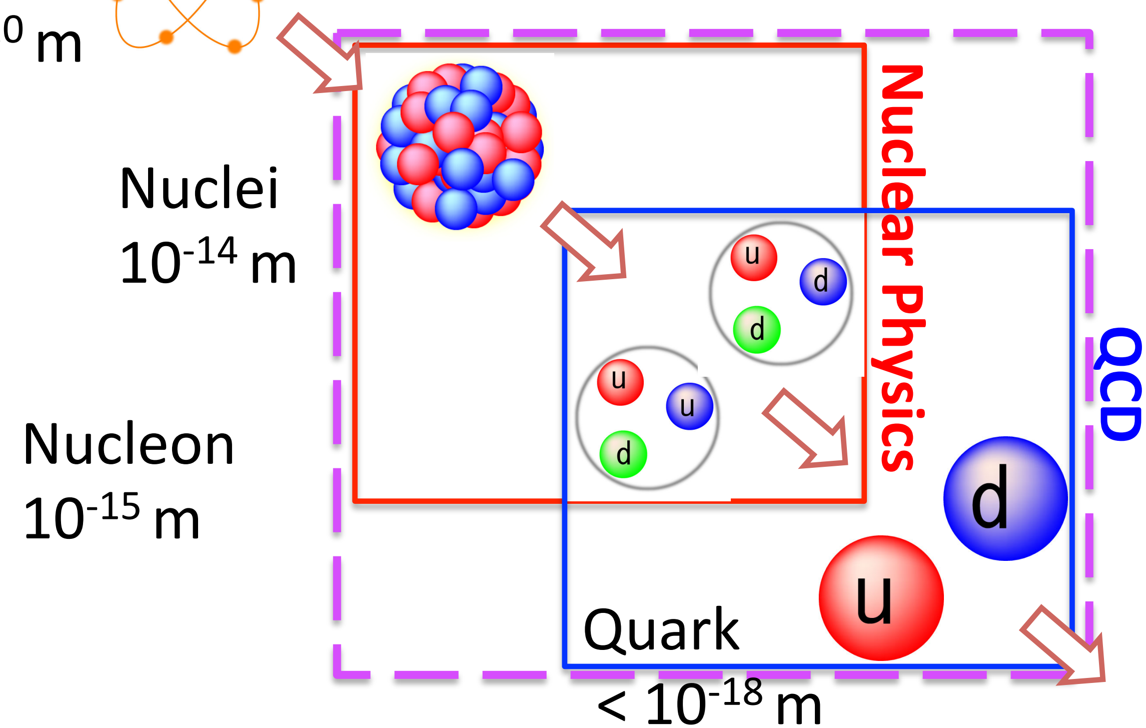

Lattice QCD at physical point

Lattice QCD simulation at Physical point

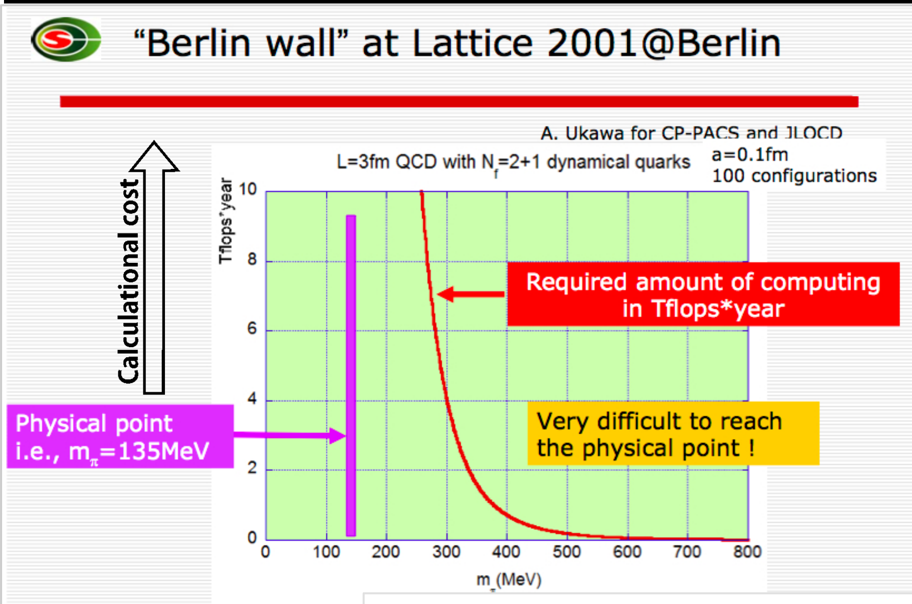

from ICRR seminar by Ukawa.

Progress of LQCD algorithm

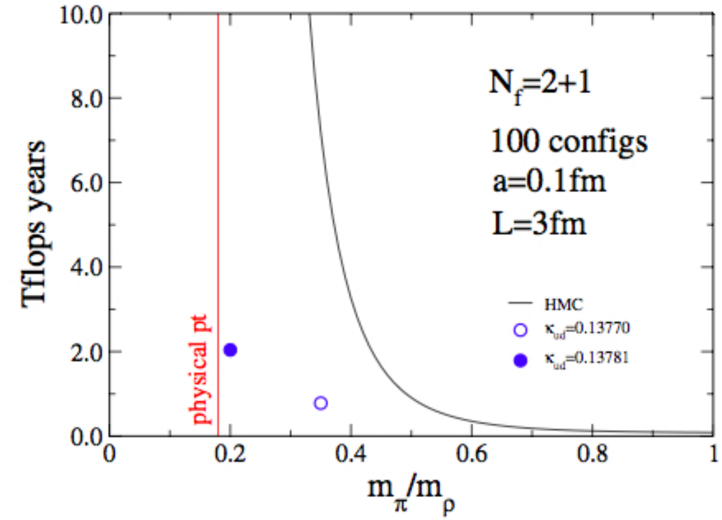

Lattice QCD simulation at the physical point is now possible.

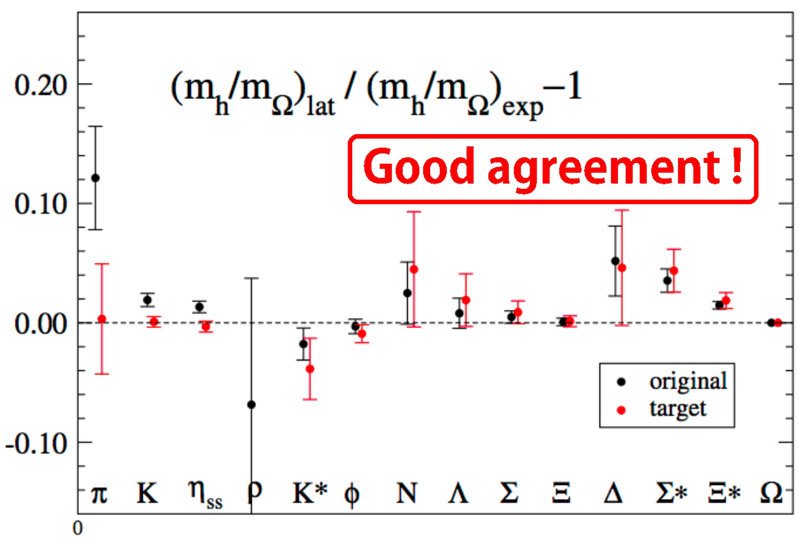

←PACS-CS, PRD81,074503(2010). [L = 3 fm]

See also:

- BMW, Science 322, 1224(2008)
- BMW, PLB701(2011)265. [L = 6fm]

Lattice QCD simulation at Physical point

- For multi-baryon systems at physical point, spatial vol. should be as huge as possible.

- Such gauge configurations have been generated by K computer.

96^4 lattice, a ∼ 0.085 fm, L ∼ 8.2 fm, m_π∼145 MeV

N.Ukita@LATTICE2015

- Determination of baryon-baryon potentials at “phys. point”.

K computer (the 4th fastest in the world)

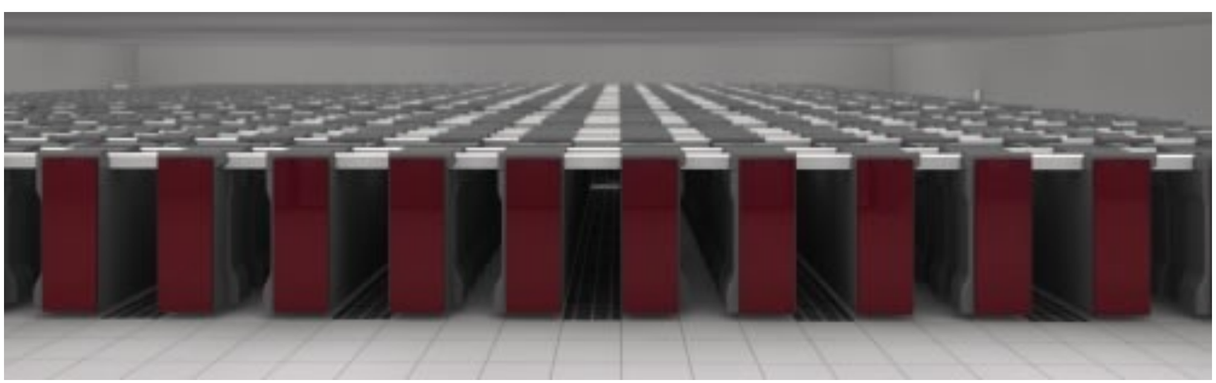

11.28 PFLOPS

Lattice QCD calculation of nuclear forces (General aspects)

HALQCD method

[Aoki,Hatsuda,Ishii,PTP123(2010)89]

◆Nambu-Bethe-Salpeter (NBS) wave func.

$$\langle 0 | T[N(x)N(y)] | N(+k)N(-k), in \rangle$$

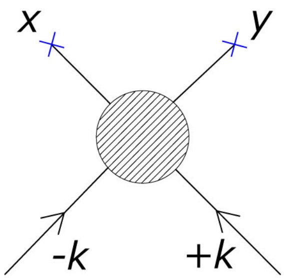

◆**Relation to S-matrix** by the reduction formula

Bosonic notation
to avoid lengthy notations.

$$\langle N(p_1)N(p_2), out | N(+k)N(-k), in \rangle_{\text{connected}}$$

$$= \left(iZ_N^{-1/2}\right)^2 \int d^4x_1 d^4x_2\, e^{ip_1x_1}\left(\Box_1 + m_N^2\right) e^{ip_2x_2}\left(\Box_2 + m_N^2\right) \langle 0 | T[N(x_1)N(x_2)] | N(+k)N(-k), in \rangle$$

◆**Equal-time** restriction of **NBS wave func.**

[C.-J.D.Lin et al., NPB619,467(2001).]

$$\psi_k(\vec{x}-\vec{y}) \equiv \lim_{x_0 \to +0} Z_N^{-1} \langle 0 | T[N(\vec{x}, x_0)N(\vec{y}, 0)] | N(+k)N(-k), in \rangle$$

$$= Z_N^{-1} \langle 0 | N(\vec{x}, 0)N(\vec{y}, 0) | N(+k)N(-k), in \rangle$$

$$\simeq e^{i\delta(k)} \frac{\sin(kr + \delta(k))}{kr} + \cdots \quad \text{as } r \equiv |\vec{x}-\vec{y}| \to \text{large}$$

(for S-wave)

❖ Exactly the same func. form as scat. wave func's in Q.M.

HALQCD method: Def of the potential

◆**Def.** of potential from **equal-time NBS wave func's**:

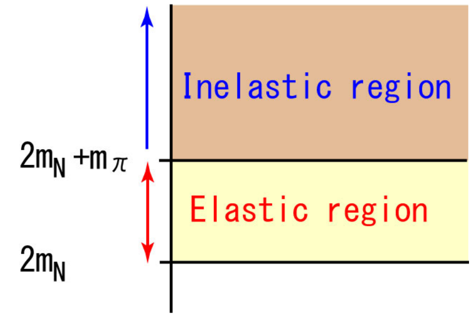

$$\left(k^2/m_N - H_0\right)\psi_k(\vec{r}) = \int d^3r' \, U(\vec{r},\vec{r}')\psi_k(\vec{r}')$$

$$\text{for } 2\sqrt{m_N^2+k^2} < E_{\text{th}} \equiv 2m_N + m_\pi$$

◆**U(r,r') is E-indep.** (One can prove its existence.)

$$H_0 \equiv -\frac{\nabla^2}{m_N}$$

◆**U(r,r') reproduces the scattering phase δ(k),**

(together with equal-time NBS wave func's)

$$\psi_k(\vec{x}-\vec{y}) \simeq e^{i\delta(k)}\frac{\sin\left(kr+\delta(k)\right)}{kr} + \cdots \quad \text{as } r \equiv \left|\vec{x}-\vec{y}\right| \to \text{large}$$

HAL QCD method

◆ **Ground state saturation becomes difficult for large spatial volume. (=single state saturation)**

$$\Delta E = E_{n+1} - E_n \sim \frac{1}{m_N}\left(\frac{2\pi}{L}\right)^2$$

$$= O\left(1/L^2\right)$$

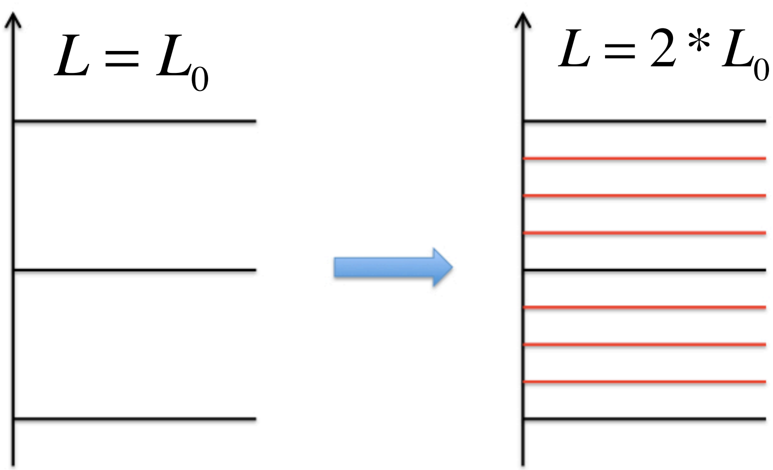

Spatial momentum is discretized due to the periodic BC.

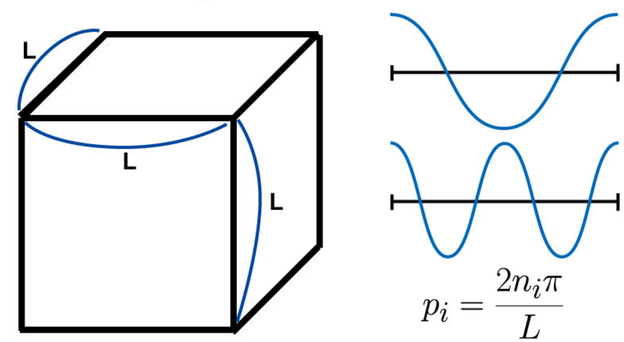

	L=3 fm	L=6 fm	L=9 fm	L=12 fm
Δ E	181.5 MeV	45.3 MeV	20.2 MeV	11.3 MeV

HAL QCD method: Determination of potentials

We have a special strategy against the ground state saturation.

◆ Def. R-correlator [Ishii et al.,PLB712(2012)437]

$$R(\vec{x}-\vec{y},t) \equiv e^{2mt} \left\langle 0 \middle| T\left[B(\vec{x},t)B(\vec{y},t)\cdot \overline{BB}(t=0)\right] \middle| 0 \right\rangle$$

$$= \sum_n \psi_{k_n}(\vec{x}-\vec{y}) \cdot \exp\left(-(E_n - 2m)t\right) \cdot a_n$$

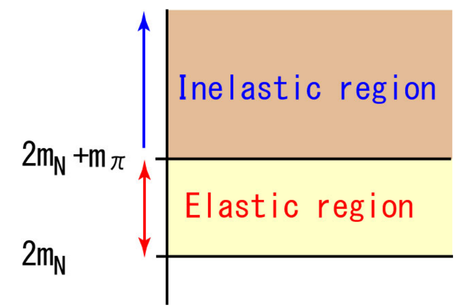

◆ HAL QCD potential satisfies Schroedinger eq.

$$\left(-H_0 + k_n^2/m\right)\psi_{k_n}(\vec{r}) = \int d^3r' V(\vec{r},\vec{r}')\, \psi_{k_n}(\vec{r}')$$

➔ R-corr. satisfies **time-dependent Schroedinger-like eq.**

$$\boxed{\left(-H_0 + \frac{1}{4m}\frac{\partial^2}{\partial t^2} - \frac{\partial}{\partial t}\right) R(\vec{r},t) = \int d^3r' V(\vec{r},\vec{r}') R(\vec{r}',t)}$$

- ☐ Only **Elastic saturation** is needed.
  Ground state saturation is not needed.
- ☐ **Elastic saturation** is much easier than **single state saturation**.

HALQCD method

◆The ground state saturation is not needed.

$$\langle 0|T[N(\vec{x},t)N(\vec{y},t)\cdot\overline{NN}(t=0;\alpha)]|0\rangle = \sum_n \psi_n(\vec{x}-\vec{y})\cdot a_n(\alpha)\cdot\exp(-E_n t)$$

$$V_C(\vec{x}) = -\frac{H_0 R(t,\vec{x})}{R(t,\vec{x})} - \frac{(\partial/\partial t)R(t,\vec{x})}{R(t,\vec{x})} + \frac{1}{4m_N}\frac{(\partial/\partial t)^2 R(t,\vec{x})}{R(t,\vec{x})}$$

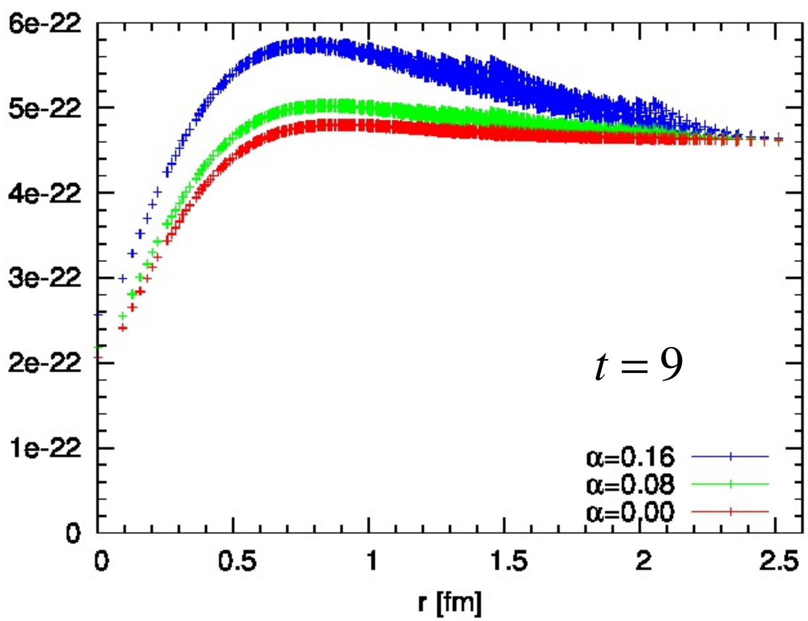

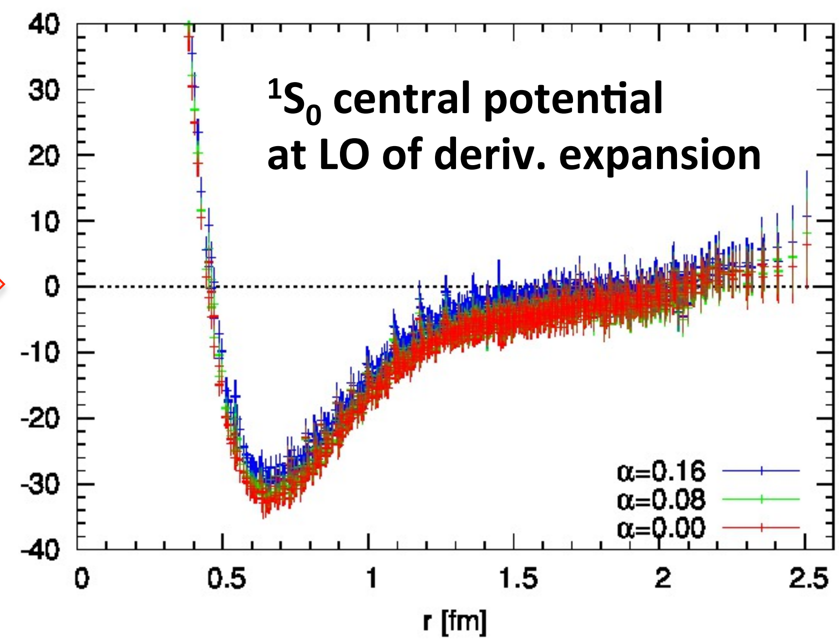

Different mixture of NBS waves are generated by different α

$$f(x,y,z) = 1 + \alpha\left(\cos(2\pi x/L) + \cos(2\pi y/L) + \cos(2\pi z/L)\right)$$

Good agreement !
➔ Our method works !

HAL QCD method

[Murano et al., PTP125(2011)1225]

◆ General nonlocal potential is messy ➔ **derivative expansion**:

$$V(\vec{r},\vec{\nabla}) \equiv V_{\mathrm{C}}(r) + \underbrace{V_{ll}(r)\vec{L}^2 + \{V_{pp}(r),\nabla^2\}}_{O(\nabla^2)\ \text{term}} + O(\nabla^4)$$

◆ The convergence of deriv.exp. is found to be good !

[Strategy to check by E-dependence]

SKIP

- We define

$$V_{\mathrm{C}}(\vec{r};E) \equiv E - \frac{H_0\psi_E(\vec{r})}{\psi_E(\vec{r})}$$

- If $V_C(r;E)$ agrees in the region $E_0 < E < E_1$

(1) We can identify

$$V_{\mathrm{C}}(\vec{r}) = V_{\mathrm{C}}(\vec{r};E)$$

(2) $O(\nabla^2)$-term is small

$$V(\vec{r},\vec{\nabla}) = V_{\mathrm{C}}(r) + \cancel{O(\nabla^2)}$$

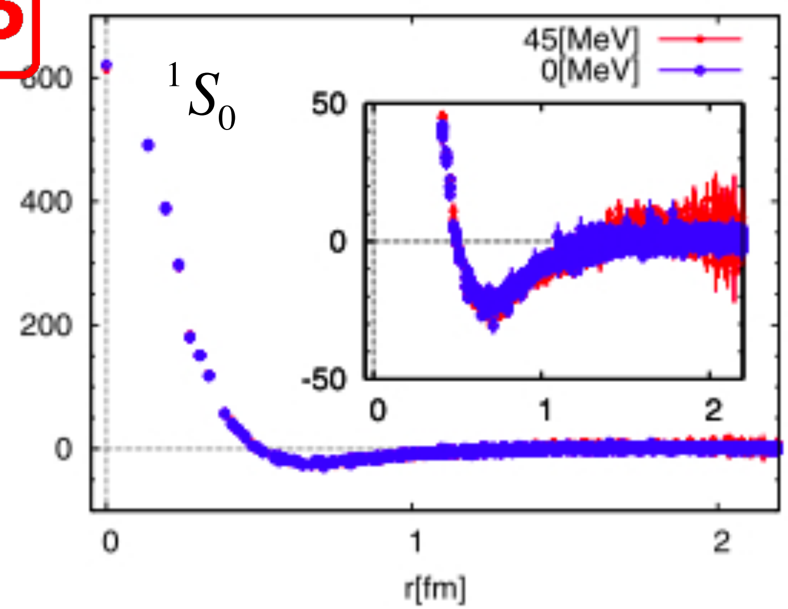

good agreement ! ➔ good convergence

Comment: The current result is obtained based on an older method.
The result should be replaced by the new method. "time-dependent" Schrodinger-like eq.

HAL QCD method

◆ Comparison of **HAL QCD method** and **Luescher's finite vol. method**

ππ scattering (I=2)

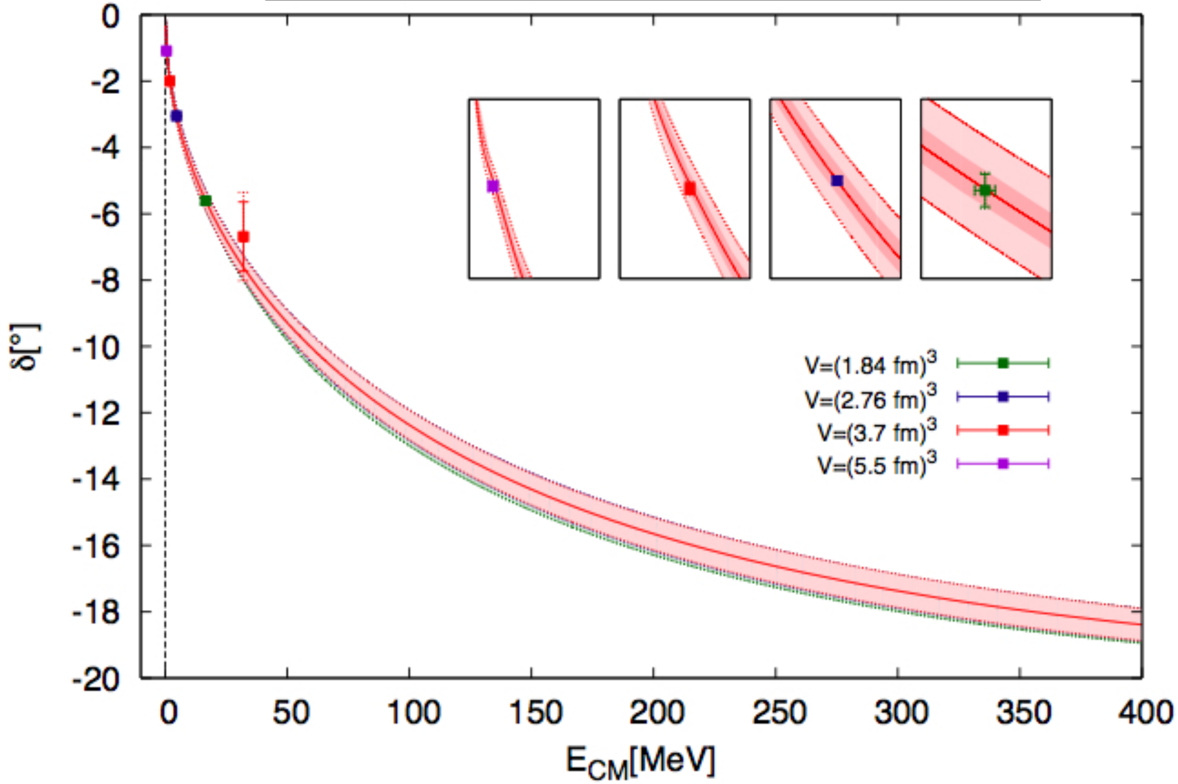

Ns=16,24,32,48, Nt=128, a=0.115 fm.
m_{pi} = 940 MeV by Quenched QCD

Good agreement !

[Kurth et al., JHEP **1312**(2013)015.]

Nuclear Forces

Nuclear Forces

◆Nuclear Force at LO (parity-even sector):

$$V_{NN} = V_{\mathrm{C;S=0}}(r)\mathbb{P}^{(S=0)} + V_{\mathrm{C;S=1}}(r)\mathbb{P}^{(S=1)} + V_{\mathrm{T}}(r)S_{12} + O(\nabla)$$

◆2+1 flavor QCD result of nuclear forces for m_π=570 MeV.

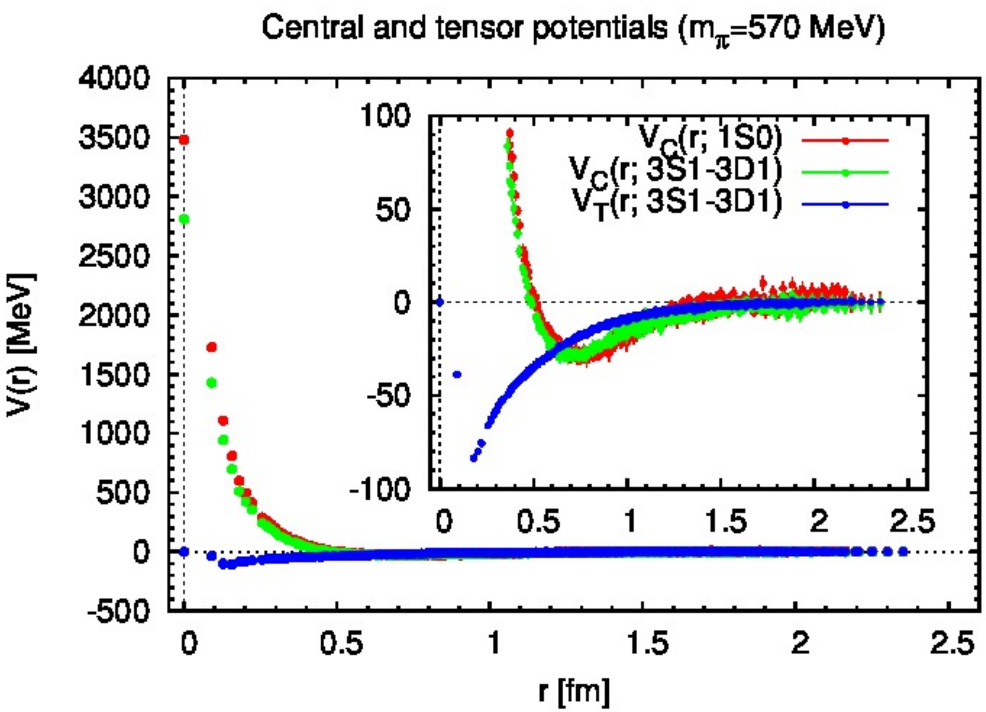

Japan Lattice Data Grid

2+1 flavor config
by PACS-CS Coll.
m(pion) = 570 MeV
m(N)=1412MeV

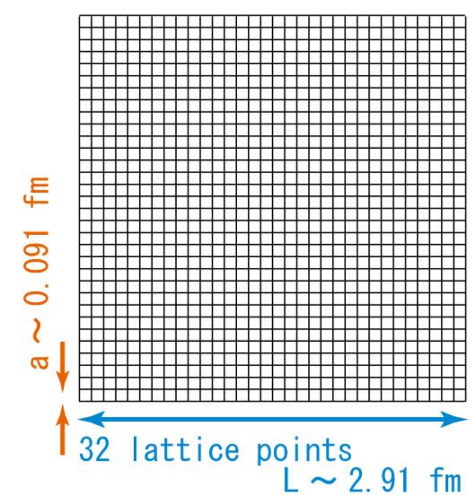

Qualitative behavior is good !
(Note: Quark mass is heavy)

Nuclear Forces

[Ishii,PoS(CD12)(2013)025]

Fit

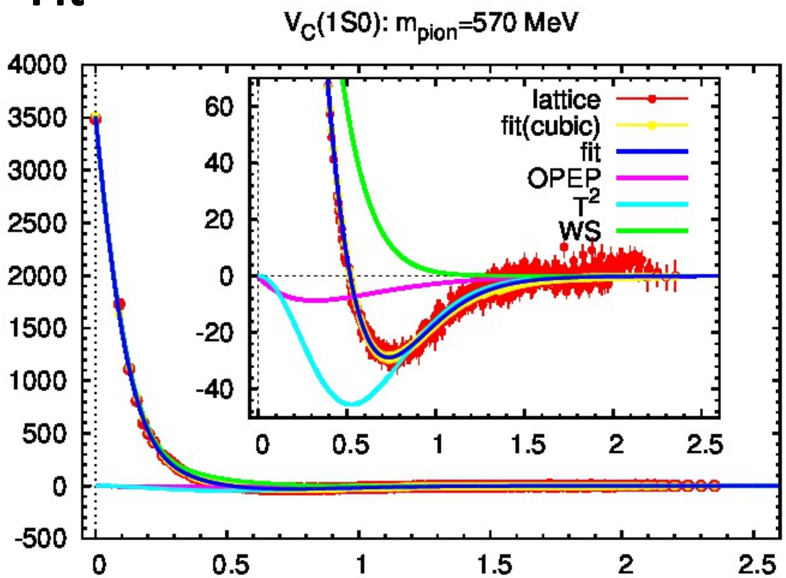

Schroedinger eq.

$^1S_0$ phase shift from Schrodinger eq.

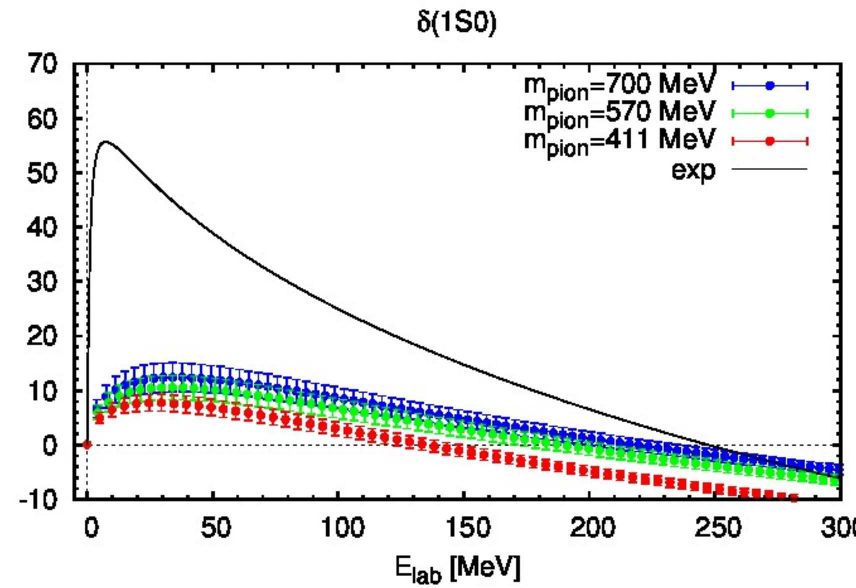

- ❖ Qualitatively good !
  (Attractive. No bound state.)

  But significantly weak.

- ❖ Attraction shrinks as m_π decreases.
  <u>Reason:</u>
  Repulsive core grows more rapidly than **attractive pocket** in the region m_{pion} = 411-700 MeV.

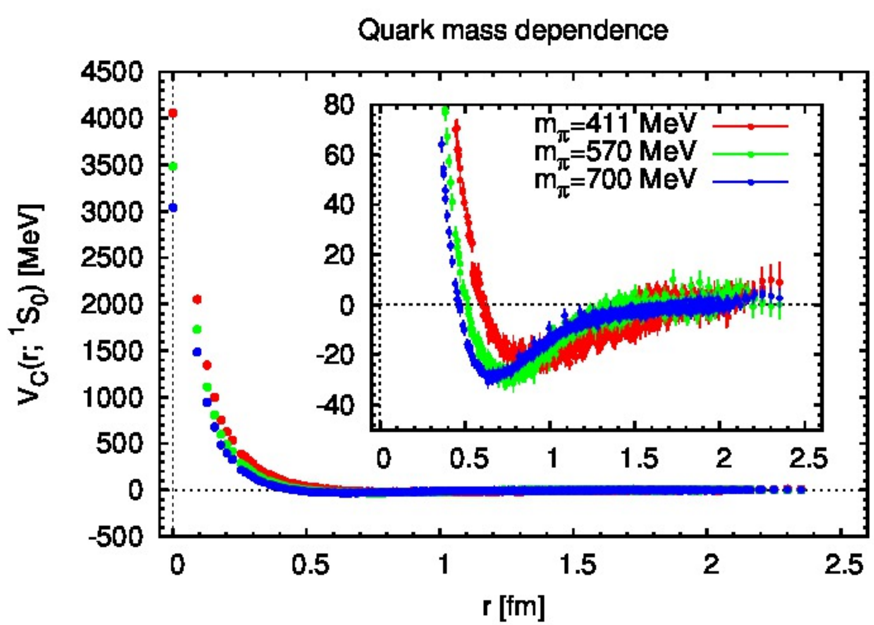

Nuclear Forces

- Three-nucleon force is important in phenomenology
  - Quantitative understanding of nuclear spectra

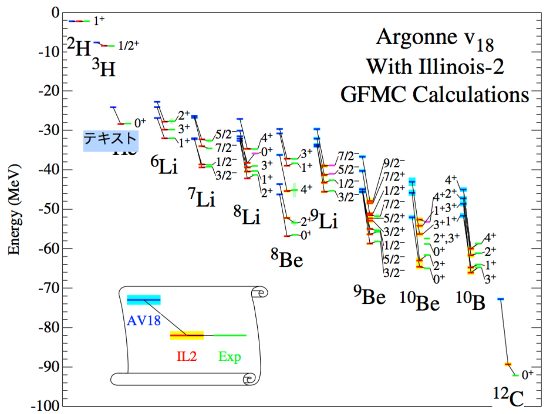

Fig. 3. – GFMC computations of energies for the AV18 and AV18+IL2 Hamiltonians compared with experiment.

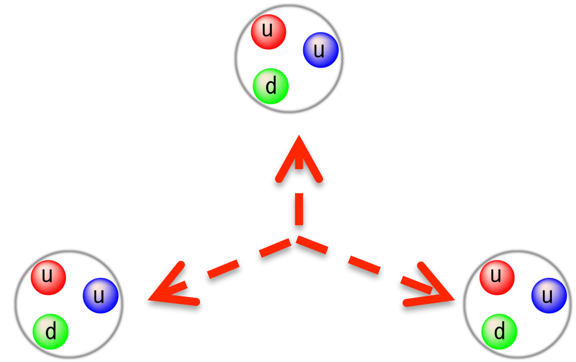

  - Astrophysical applications: Neutron star and Super nova

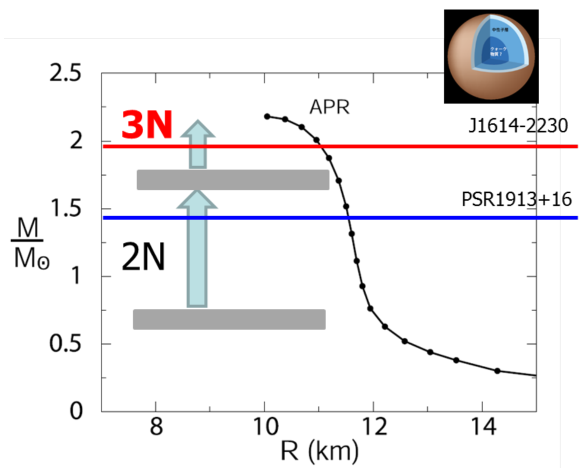

- Experimental information is limited

Nuclear Forces

[T.Doi et al, PTP127,723(2012)]

◆ Three-nucleon potential (on the linear setup)

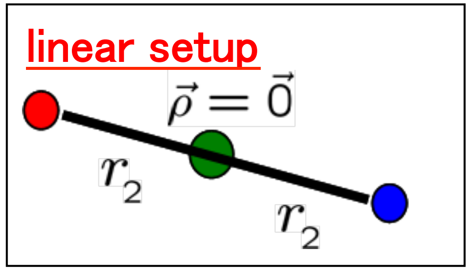

2 flavor gauge config by CP-PACS Coll.
m(pion) = 1136 MeV, m(N) = 2165 MeV

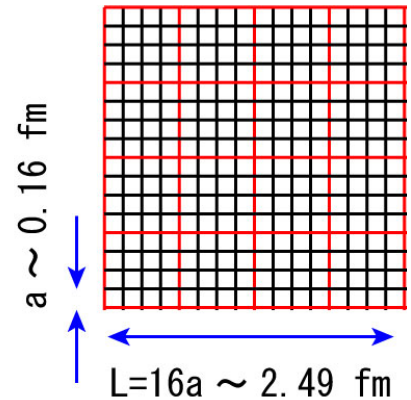

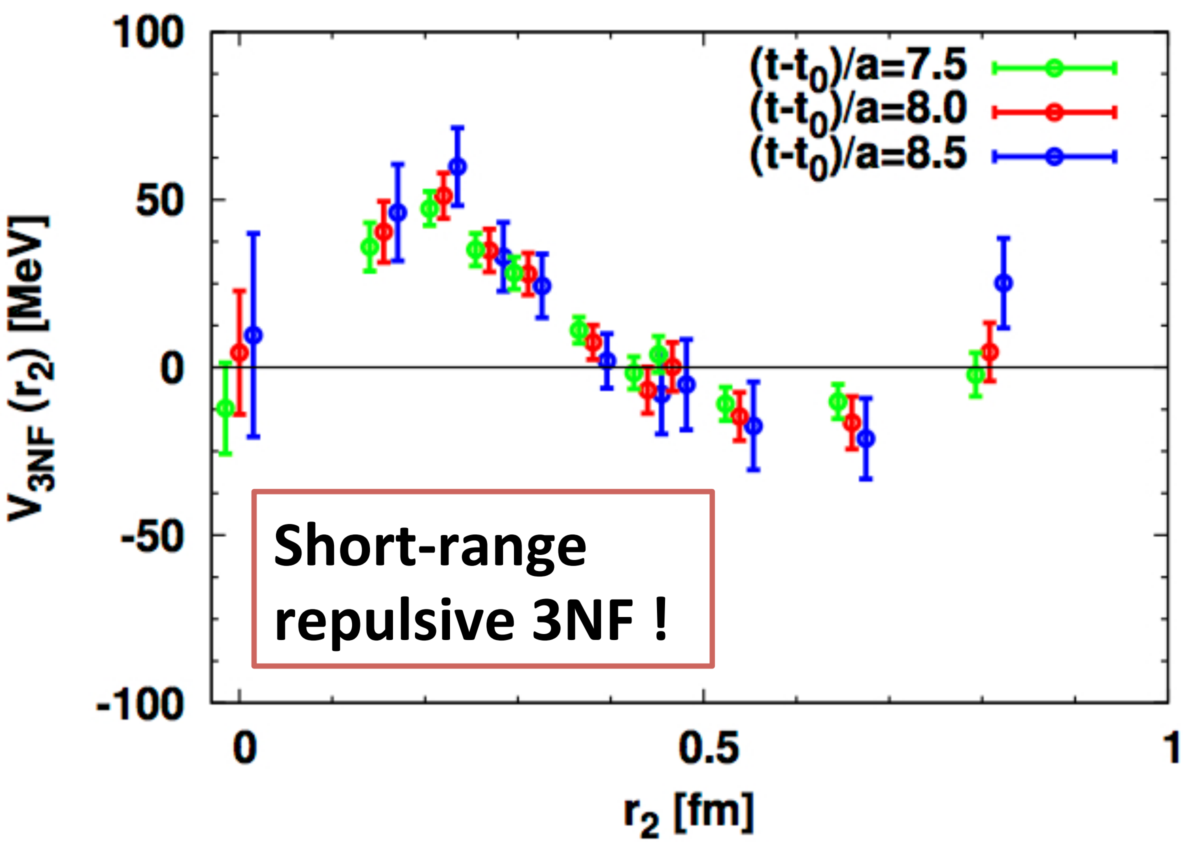

Nuclear Forces

◆Nuclear Force up to NLO

$$V^{(\pm)}(\vec{r},\vec{\nabla}) = \underbrace{V^{(\pm)}_{\mathrm{C;S=0}}(r)\mathbb{P}^{(S=0)} + V^{(\pm)}_{\mathrm{C;S=1}}(r)\mathbb{P}^{(S=1)} + V^{(\pm)}_{\mathrm{T}}(r)S_{12}(\hat{r})}_{\mathrm{LO}:O(\nabla^0)} + \underbrace{V^{(\pm)}_{\mathrm{LS}}(r)\vec{L}\cdot\vec{S}}_{\mathrm{NLO}:O(\nabla^1)} + O(\nabla^2)$$

◆**Spin orbit (LS) force** is important in phenomenology.

Magic number (nuclei)

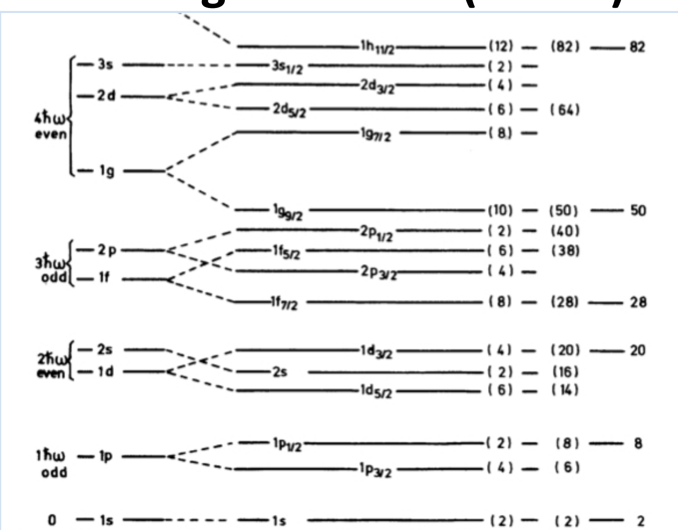

$^3P_2$ neutron superfuluid (neutron star cooling)

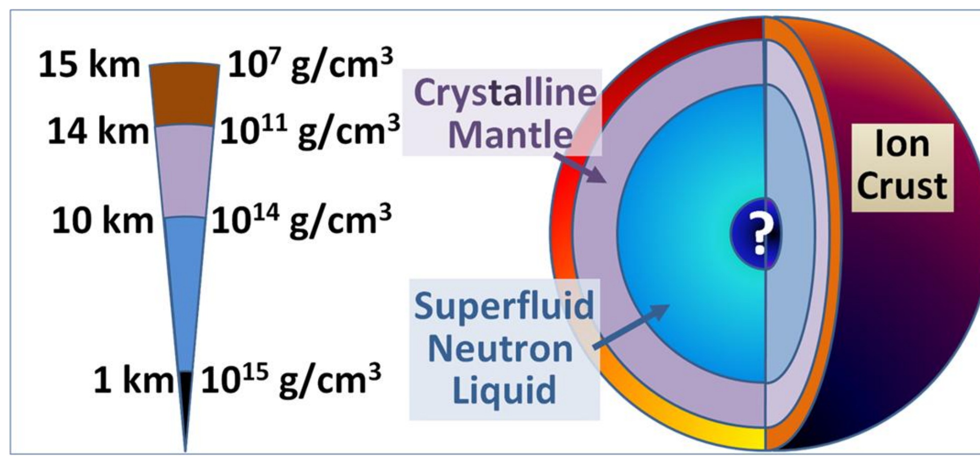

Nuclear Forces

[K.Murano et al., PLB735(2014)19.]

◆ Nuclear forces and **LS force** in **parity-odd** sector

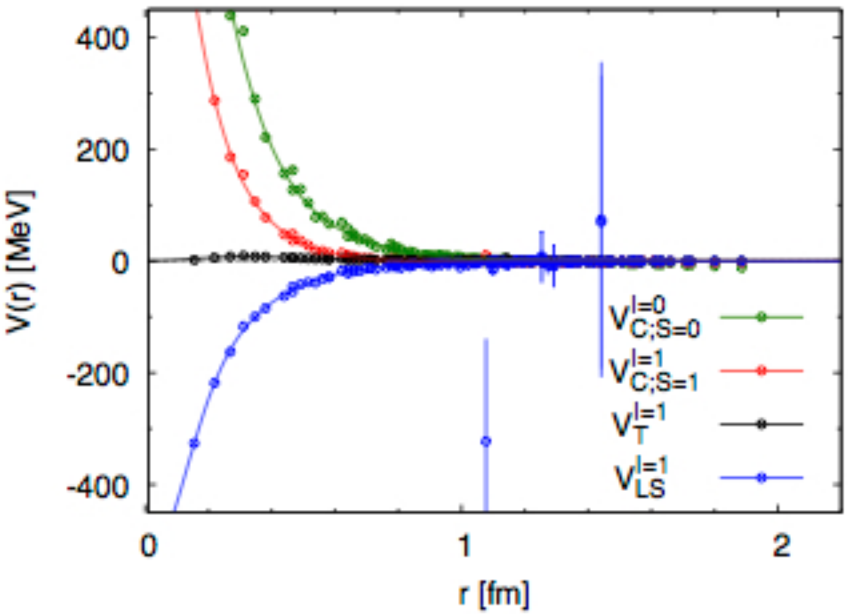

AV18 for comparison

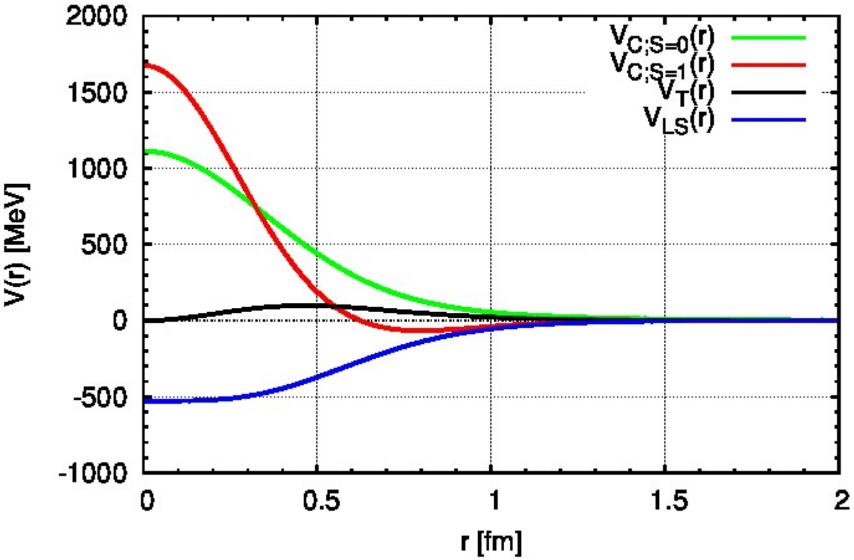

Scattering phase shifts

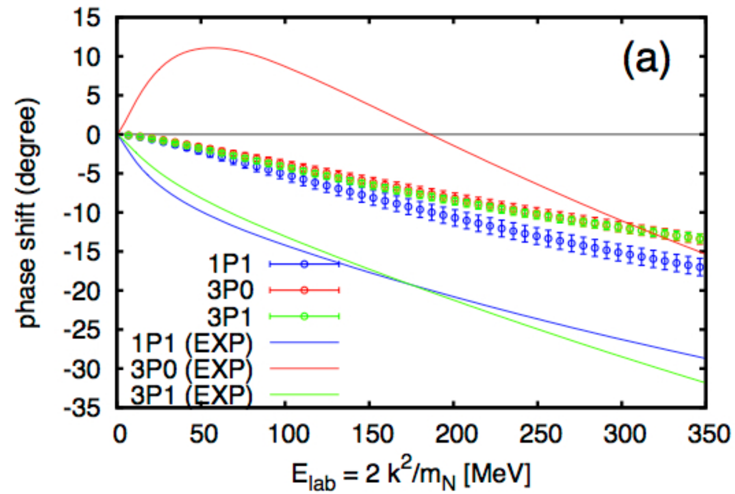

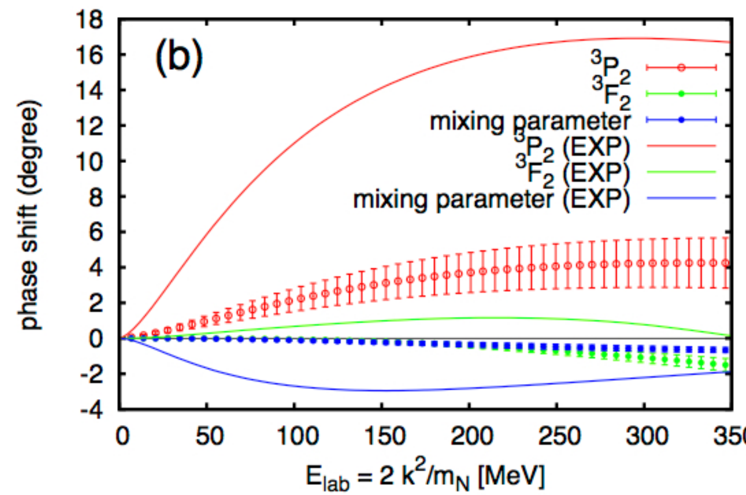

◆ Qualitatively good

◆ Strength is weak

Potential method and direct method

Potential method and direct method

[T.Doi, PoS LAT2012,009]

◆ A conflict in LQCD calculation of NN in heavy quark mass region.

"di-neutron"

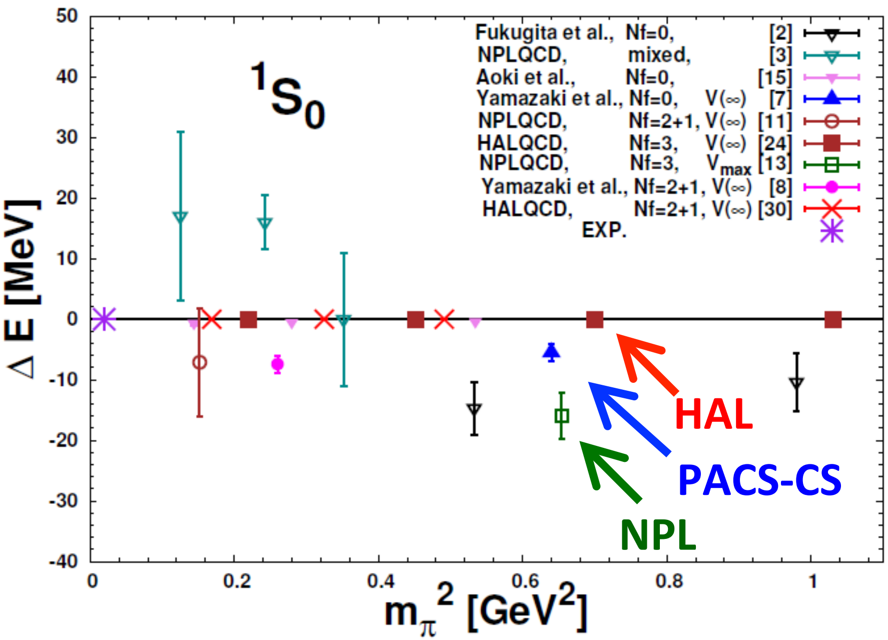

"deuteron"

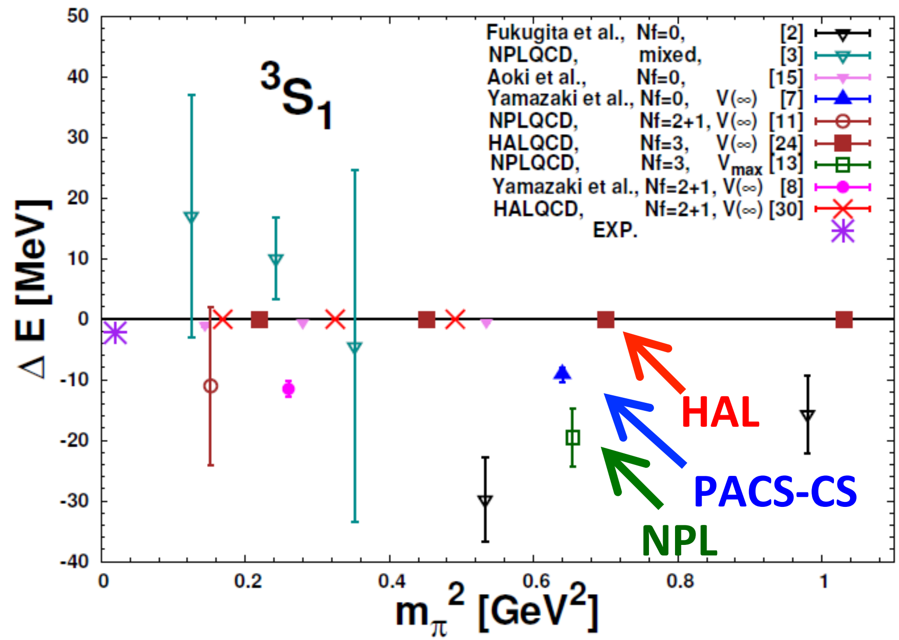

◆ **PACS-CS Coll. & NPL QCD Coll.**
- ❖ attractive both for $^1S_0$ & $^3S_1$
- ❖ bound states both for $^1S_0$ & $^3S_1$
- ❖ direct method
- ❖ smearing source

◆ **HAL QCD Coll.**
- ❖ attractive both for $^1S_0$ & $^3S_1$
- ❖ no bound states both for $^1S_0$ & $^3S_1$
- ❖ potential method
- ❖ wall source

Potential method and direct method

◆We compare these two methods

□ **potential method (HAL QCD method)**

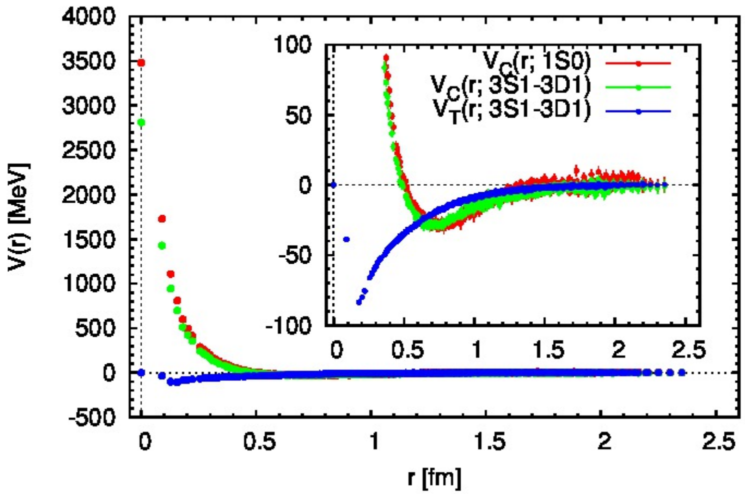

□ **direct method**

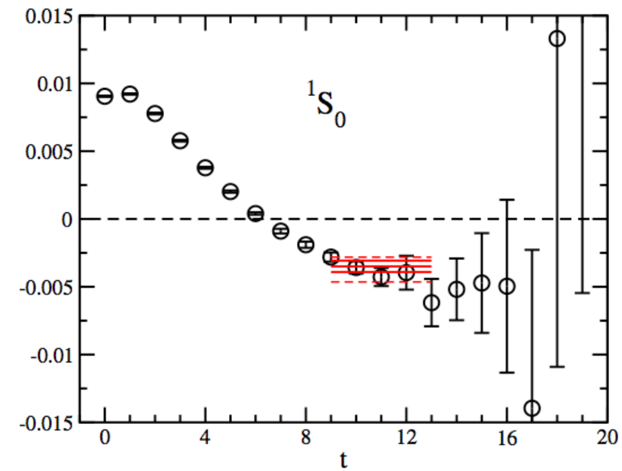

Fig. Yamazaki et al. '15

We use the same gauge config's as Yamazaki et al., PRD86,074514; PRD92,014501.

volume	conf.	smared src. meas.	wall src. meas.
$40^3 \times 48$	200	192	48
$48^3 \times 48$	800	256	48
$64^3 \times 64$	327	48	32

Table: Lattice configurations (we mainly use $48^3 \times 48$ volume)

$$m_\pi = 0.51\mathrm{GeV},\ m_N = 1.32\mathrm{GeV}, m_K = 0.62\mathrm{GeV}, m_\Xi = 1.46\mathrm{GeV}$$

❖ ΞΞ channel is used for statistical reason.

Potential method and direct method

[T.Iritani@LATTICE2015]

- Key role is played by R-correlator:

$$R(\vec{r},t) \equiv C_{\Xi\Xi}(\vec{r},t) / C_{\Xi}(t)^2$$

- direct method

$$R(t) \equiv \sum_{\vec{r}} R(\vec{r},t) = \sum_n a_n \exp\left(-\Delta E_n t\right) \Rightarrow \Delta E = E_{\Xi\Xi} - 2m_{\Xi}$$

- potential method

$$\left(\frac{1}{4m}\frac{\partial^2}{\partial t^2} - \frac{\partial}{\partial t} - H_0\right) R(\vec{r},t) = \int d^3r' \, V(\vec{r},\vec{r}') R(\vec{r}',t)$$

- R(r,t): smearing src. v.s. wall src.

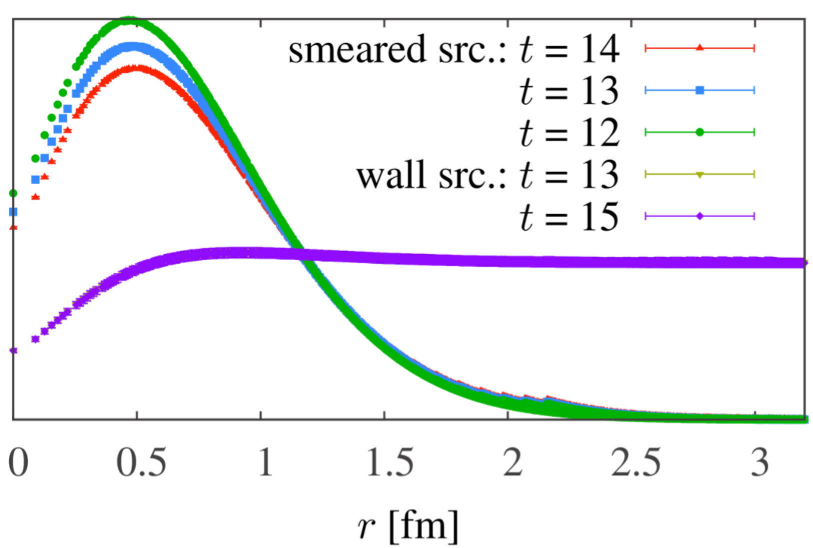

- smearing source:
  Shape changes with t.

- wall source:
  Shape change less significant.

Potential method and direct method

◆Effective mass plot of

$$R(t) \equiv C_{\Xi\Xi}(t) \,/\, C_{\Xi}(t)^2$$

- Be careful with effective mass plot
  $\Rightarrow$ fictious "plateau" appears

- ○ at least $t \gtrsim 16$
- ○ smared src. m_Ξ tends to large

$\Delta E = M_{\Xi\Xi} - 2m_\Xi$

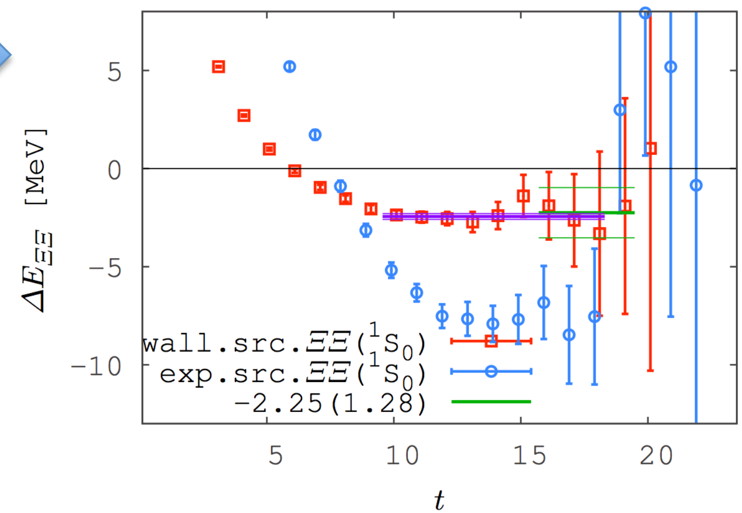

Effective mass plot of $C_{\Xi\Xi}(t)$

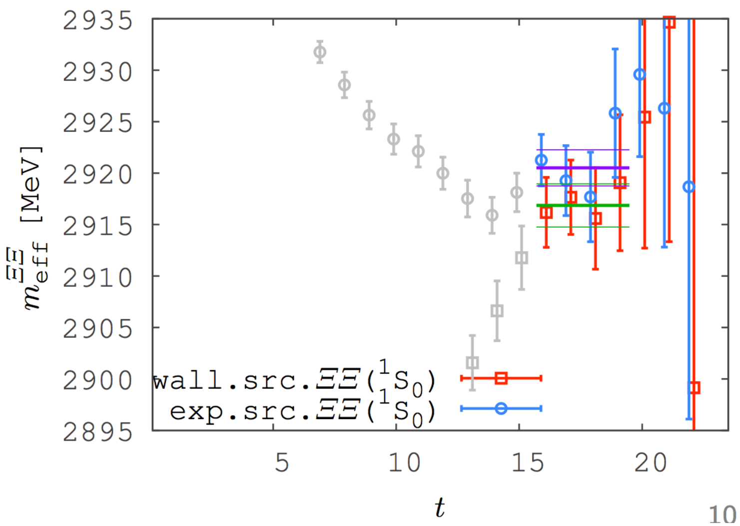

Effective mass plot of $C_{\Xi}(t)$

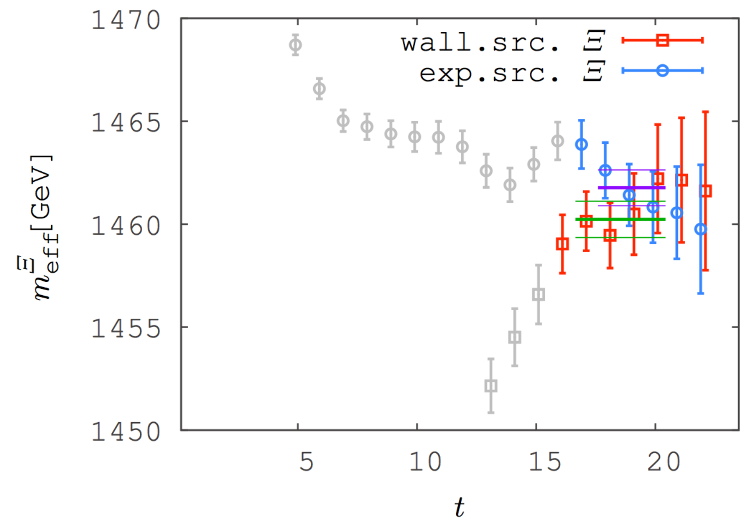

Potential method and direct method

- Potential construction by t-dep. HAL QCD method

> - time-dep. method works
>
> $$V(\vec{r}) = -\frac{H_0 R(\vec{r},t)}{R(\vec{r},t)} - \frac{(\partial/\partial t)R(\vec{r},t)}{R(\vec{r},t)} + \frac{(\partial/\partial t)^2 R(\vec{r},t)}{4m R(\vec{r},t)}$$
>
> ☐ **wall src.:**
> these three terms add up.
>
> ☐ **smearing src.:**
> After a "miracle" cancellation of these three terms, they add up to give a similar shape.

wall src.

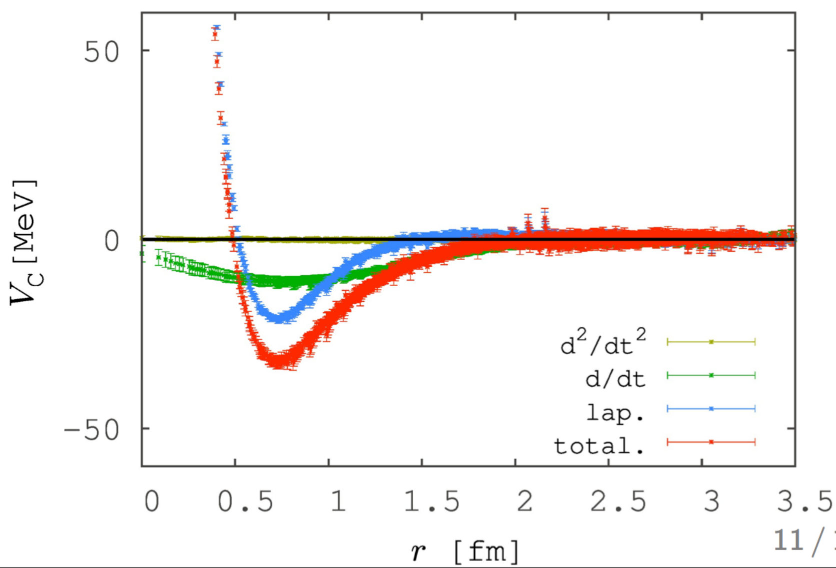

smeared src.

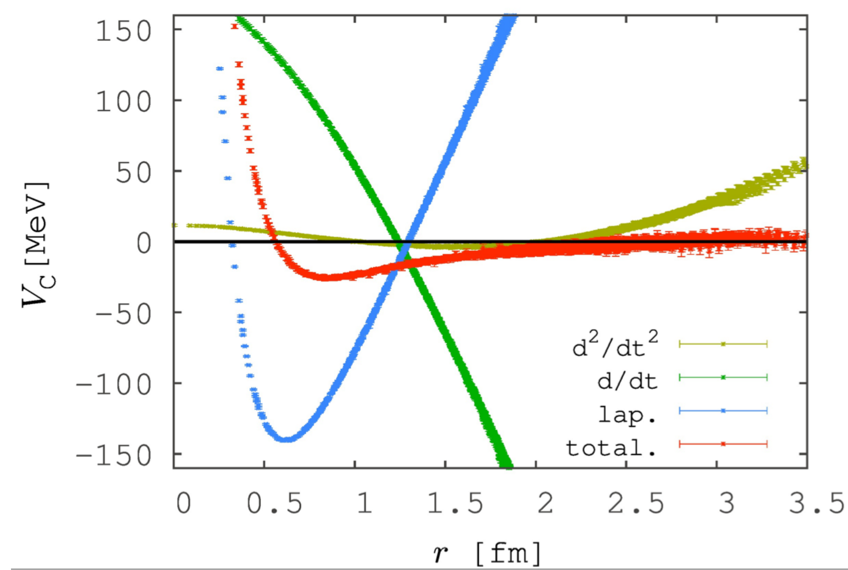

Potential method and direct method

[T.Iritani@LATTICE2015]

◆ Potentials from **smearing source** and **wall source**

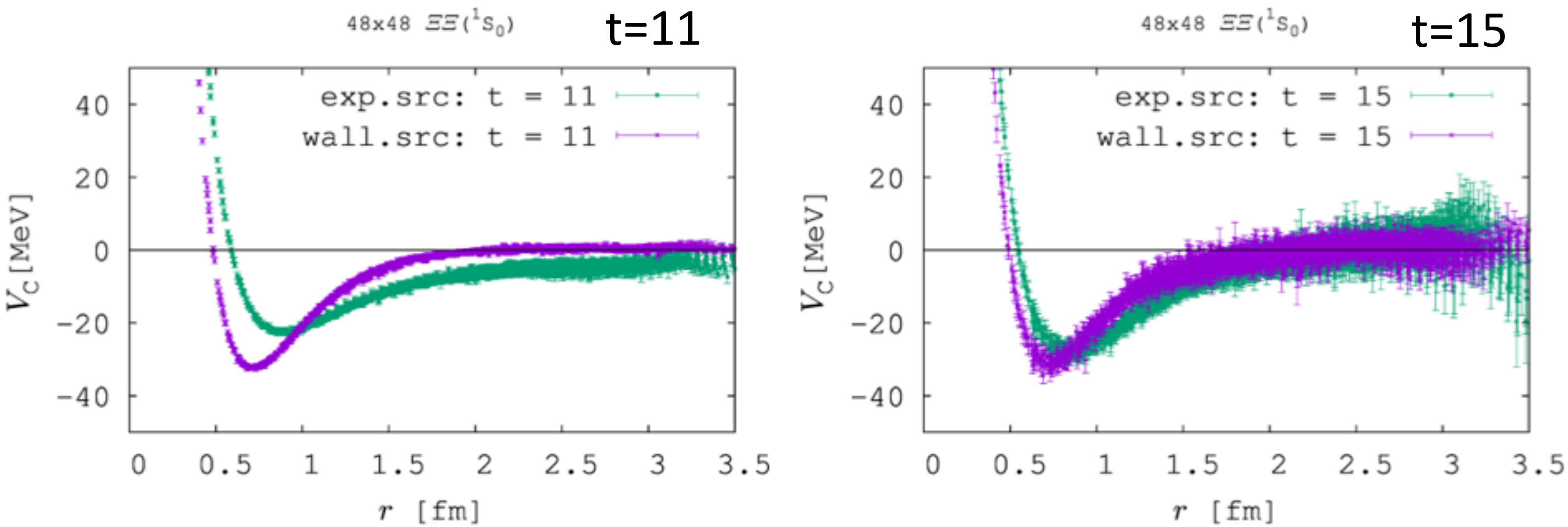

❖ There is a deviation.

❖ **potential from wall src.** does not have t-dependence.
potential from smearing src. has t-dependence.

❖ As t→large, **smearing src. result** tends to converge to **wall src. result**.

❖ Deviation is due to the NLO in derivative expansion. (➔ NEXT SLIDE)

$$U(\vec{r},\vec{r}') = \left(V_0(\vec{r}) + V_1(\vec{r})\nabla^2 + \cdots\right)\delta^3(\vec{r}-\vec{r}')$$

Potential method and direct method

[T.Iritani (NEW)]

SKIP

◆ Determination of NLO potential

$$V(\vec{r},\nabla) = V_0(\vec{r}) + V_1(\vec{r})\nabla^2 + \cdots$$

$$\begin{cases} V_0(r)R(\vec{r},t';\mathcal{J}_{\text{wall}}) + V_1(r)\nabla^2 R(\vec{r},t';\mathcal{J}_{\text{wall}}) = V_{\text{total}}^{\text{wall}}(r) \equiv \left(\dfrac{1}{4m}\dfrac{\partial^2}{\partial t'^2} - \dfrac{\partial}{\partial t'} - H_0\right) R(\vec{r},t';\mathcal{J}_{\text{wall}}) \\[2ex] V_0(r)R(\vec{r},t;\mathcal{J}_{\text{smear}}) + V_1(r)\nabla^2 R(\vec{r},t;\mathcal{J}_{\text{smear}}) = V_{\text{total}}^{\text{smear}}(r) \equiv \left(\dfrac{1}{4m}\dfrac{\partial^2}{\partial t^2} - \dfrac{\partial}{\partial t} - H_0\right) R(\vec{r},t;\mathcal{J}_{\text{smear}}) \end{cases}$$

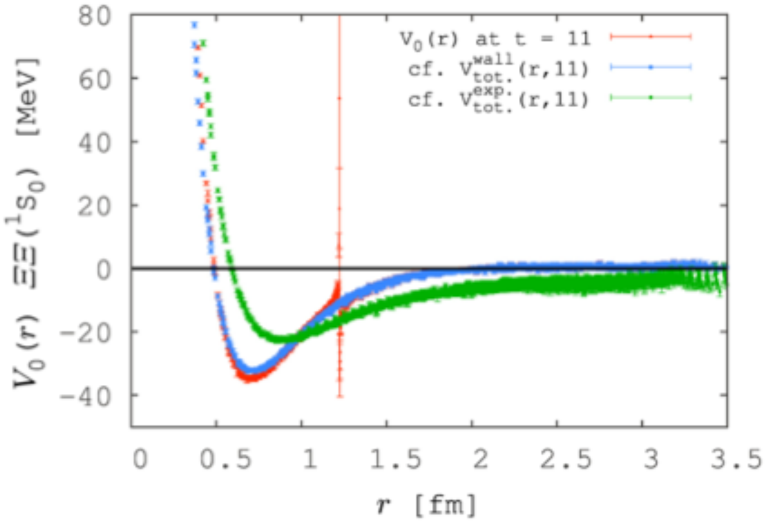

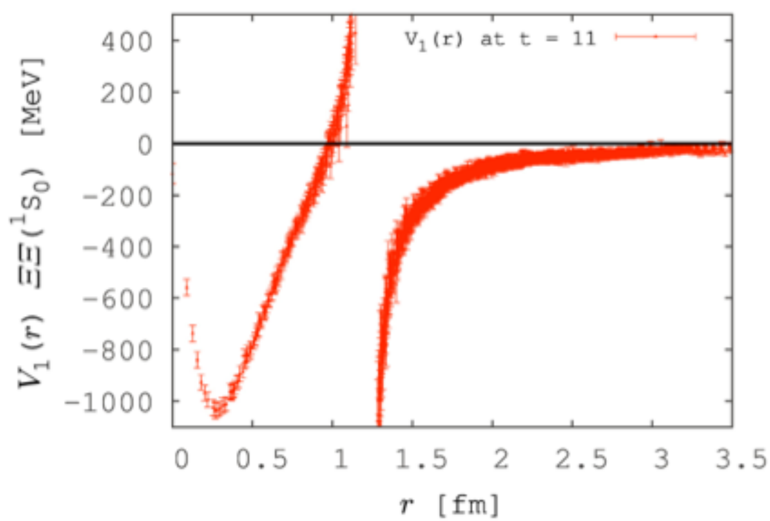

◆ $V_{\text{total}}^{\text{wall}}(r)$ and $V_{\text{total}}^{\text{smear}}(r)$ are parameterized by $V_0(r)$ and $V_1(r)$.

◆ **Wall src**: Deriv. exp. up to LO works: $V(\vec{r},\nabla) \simeq V_0(\vec{r}) + \cancel{V_1(\vec{r})\nabla^2} + \cdots$

◆ **smearing src: NLO is needed** : $V(\vec{r},\nabla) \simeq V_0(\vec{r}) + V_1(\vec{r})\nabla^2 + \cdots$

Potential method and direct method

[T.Iritani@LATTICE2015]

◆“Potential method” is consistent with the “direct method”

“wall source” at $t = 12$

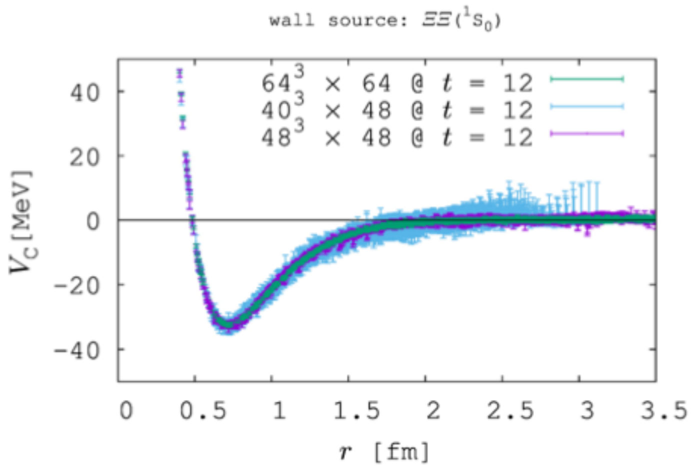

- Now, we have the potential $V_c^{\Xi\Xi}(\vec{r})$

$\Rightarrow$ solve “finite volume” eigen energies†

- consistent with “wall src.” $\Delta E(t)$ fit $-2.25(1.28)$ MeV @ $48^3 \times 48$
- vol. dep. implies scattering states

energy eigenvalues

vol.	E(g.s.) [MeV]	E(1st) [MeV]
40^3	$-4.55(1.18)$	$75.63(1.31)$
48^3	$-2.58(22)$	$52.87(33)$
64^3	$-1.13(9)$	$28.71(9)$

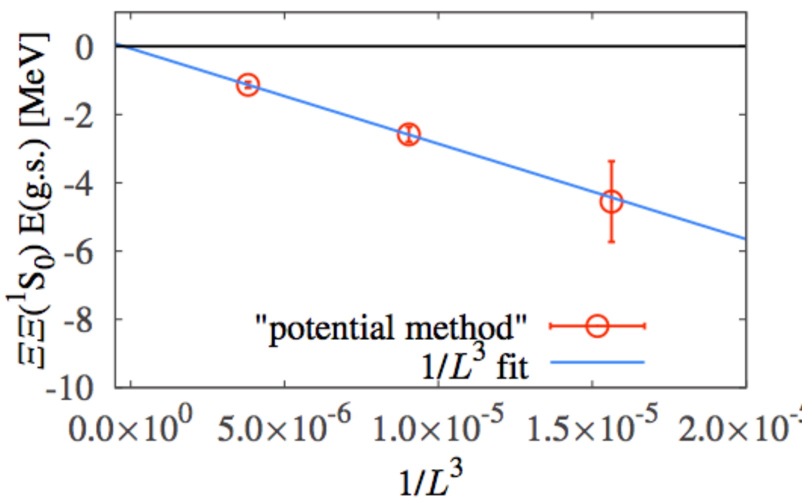

† ref. Charron for HAL QCD Coll. arXiv:1312.1032.

Potential method and direct method

◆Local summary

- Identification of **plateau** in multi-nucl. syst. should be **very careful**.
  - Many **cancellations** are involved, which can lead to **fake plateaux**.
  - **Some special technique** should be developed against this problem. (like **time-dep. method** in potential method.)

- “**Potential method**” is consistent with “**direct method**”.

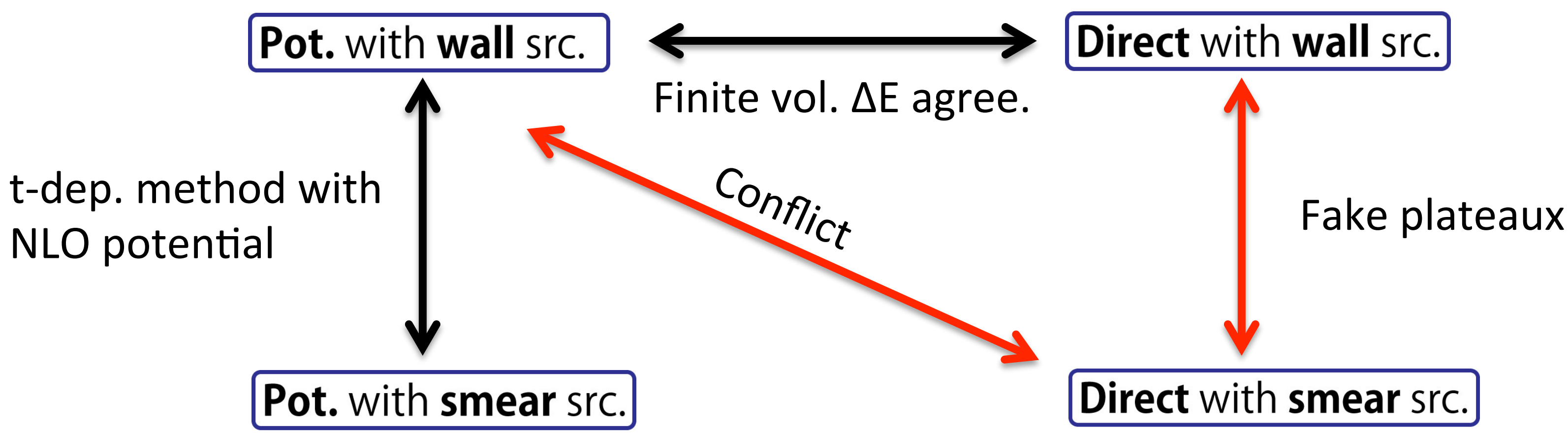

- For **direct method** with **smear src**, **systematic uncertainties** appear to be **large**.
  - ➔ Results should be checked by
    - ❖ Other method
    - ❖ Other source.

This applies to (i) Yamazaki et al. & (ii) NPL QCD

Hyperon Forces

Determination of Hyperon Forces

◆These two are complementary:

Experiment (J-PARC)

◆ **Experiment** ⇄ Fey Body ⇄ Effective models

◆ Excitation spectrum of hyper nuclei
Many body syst.→Two body pot.

◆ Easier for smaller num. of strange quarks

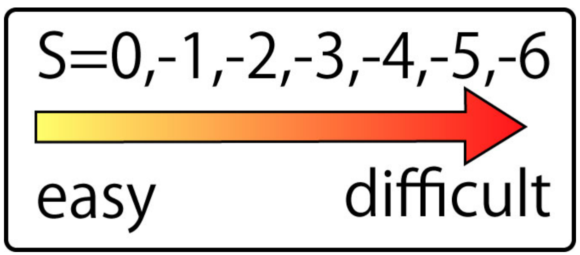

❖ Nuclear force
Huge number of experimental data
→ High precision potential

LQCD (HAL QCD method)

◆ **Theory**（LQCD with HAL QCD method）

◆ Scattering phases
Two body syst.→Two body pot.

◆ Easier for larger num. of strange quarks

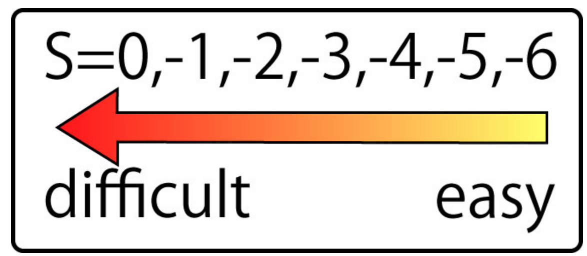

❖ Nuclear force
Large statistical noise.
→ Large computational resource

Best to collaborate
to make a high precision hyperon potentials.

Hyperon Forces

Nemura, Ishii, Aoki, Hatsuda, PLB673(2009)136.

$\Xi N(I=1)$

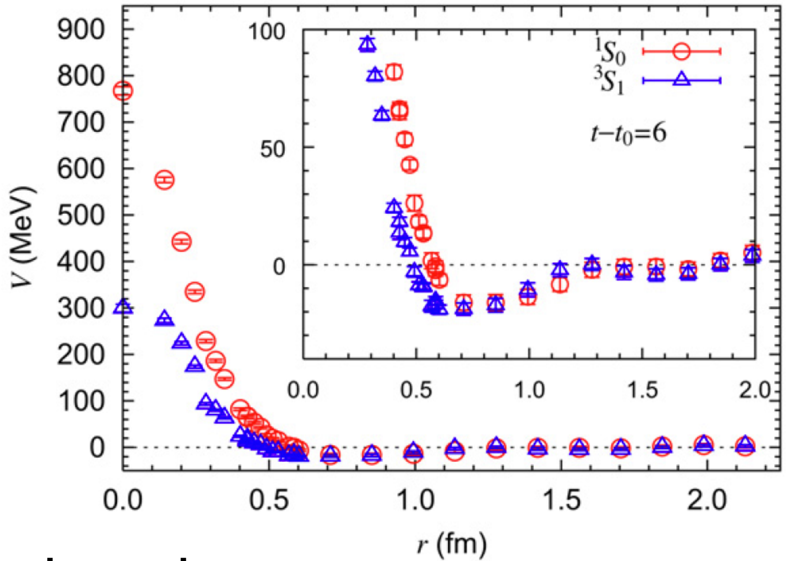

- Repulsive core is surrounded by attraction like NN case.
- Strong spin dependence of repulsive core.

quark mass dependence

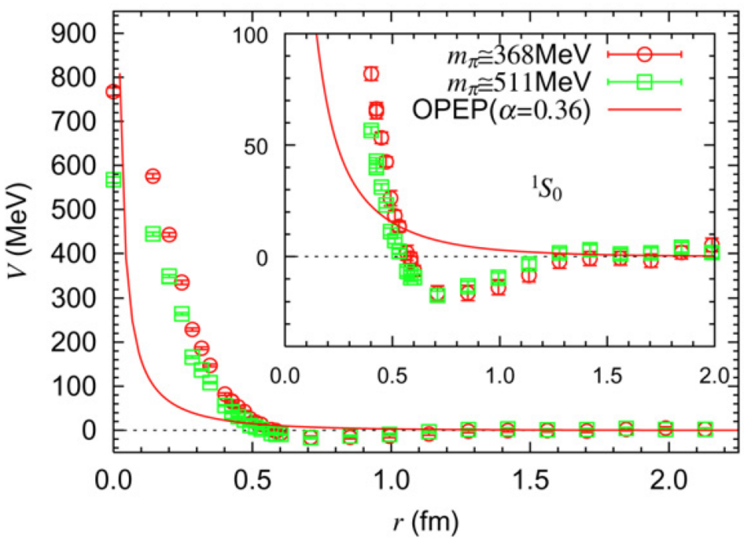

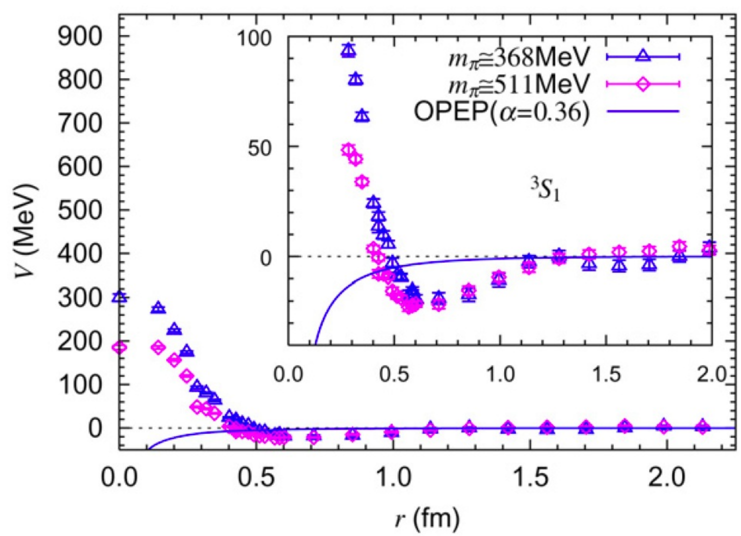

Repulsive core grows with decreasing quark mass.
No significant change in the attraction.

Hyperon Forces

Spin-singlet sector

$^1S_0$

ΛN

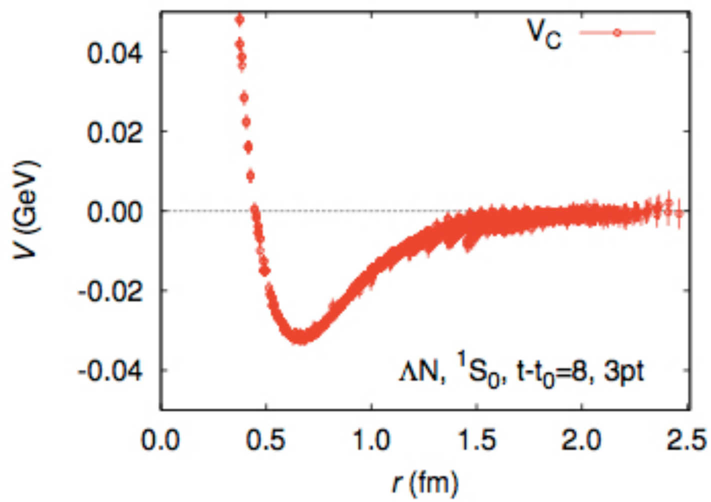

$\Sigma N(I = 3/2)$

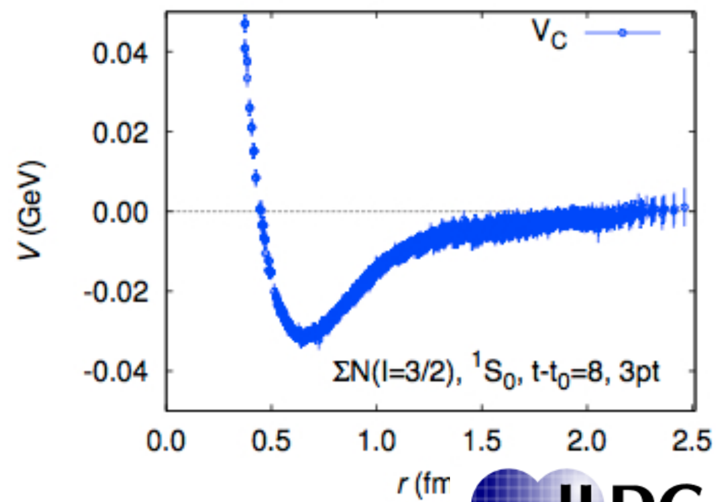

2+1 flavor config by PACS-CS Coll.
m(pion) = 570 MeV, m(N)=1412MeV

- Repulsive core is surrounded by attraction like NN case.

- These two potentials looks similar.
  (This may be due to small flavor SU(3) breaking.)

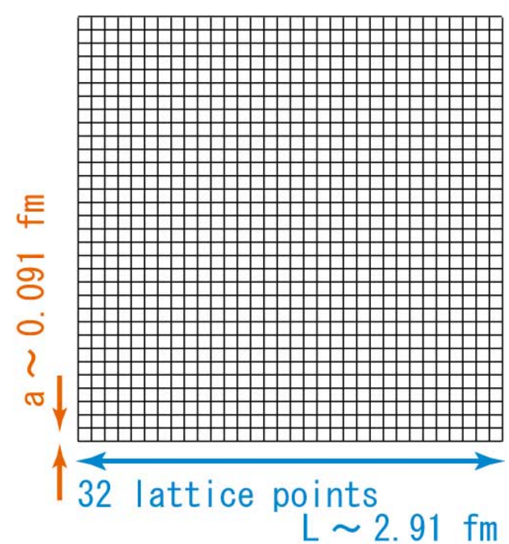

Hyperon Forces

[Nemura,PoS(LAT2011)]

Spin-triplet sector

$^3S_1 - ^3D_1$

ΛN

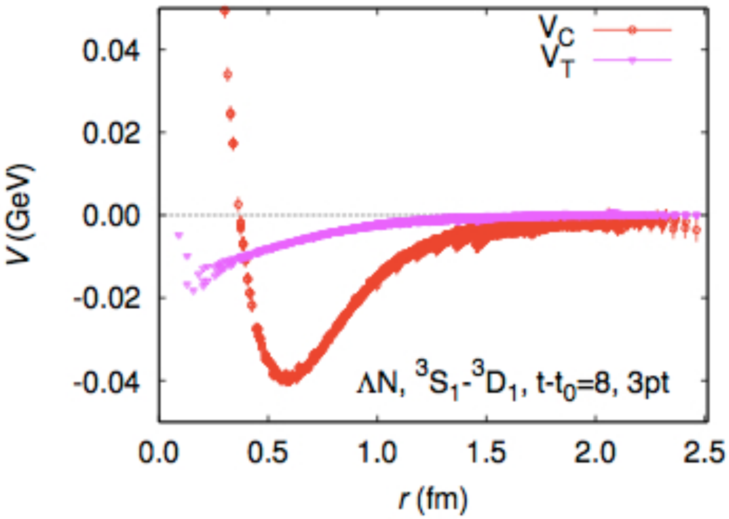

$\Sigma N(I = 3/2)$

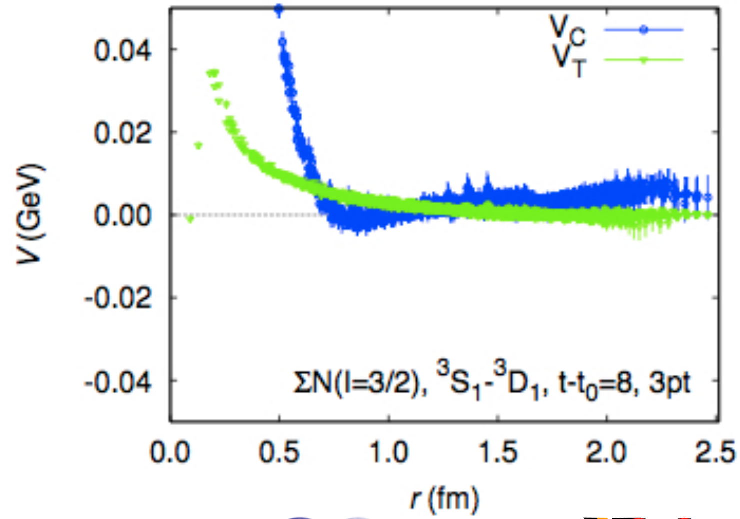

Japan Lattice Data Grid

2+1 flavor config by PACS-CS Coll.
m(pion) = 570 MeV, m(N)=1412MeV

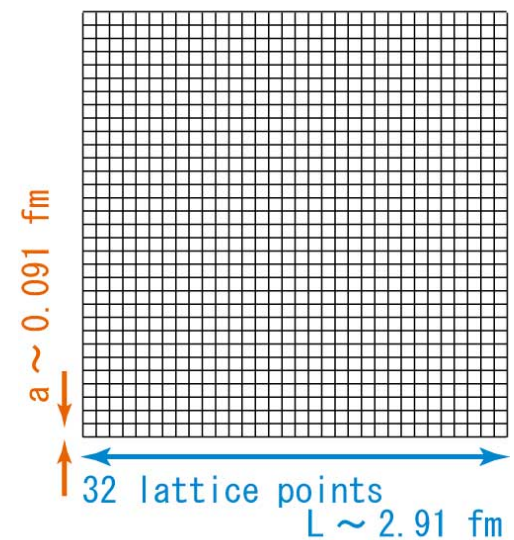

- N-Lambda
  - Repulsive core is surrounded by attraction
  - The attraction is deeper than 1S0
  - Weak tensor force (no one-pion exchange is allowed)

- N-Sigma
  - Repulsive core at short distance
  - No clear attractive well
    (Repulsive nature is consistent with the quark model)

Hyperon Forces

[T.Inoue et al, PTP124,591(2010)]

◆ **Flavor SU(3) limit** to understand a general trend

$$8 \otimes 8 = \underbrace{27 \oplus 8_S \oplus 1}_{\text{symmetric}} \oplus \underbrace{\overline{10} \oplus 10 \oplus 8_A}_{\text{anti-symmetric}}$$

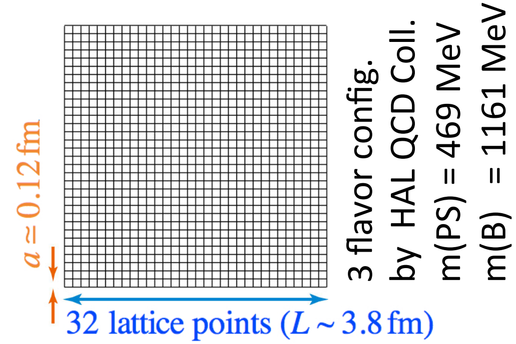

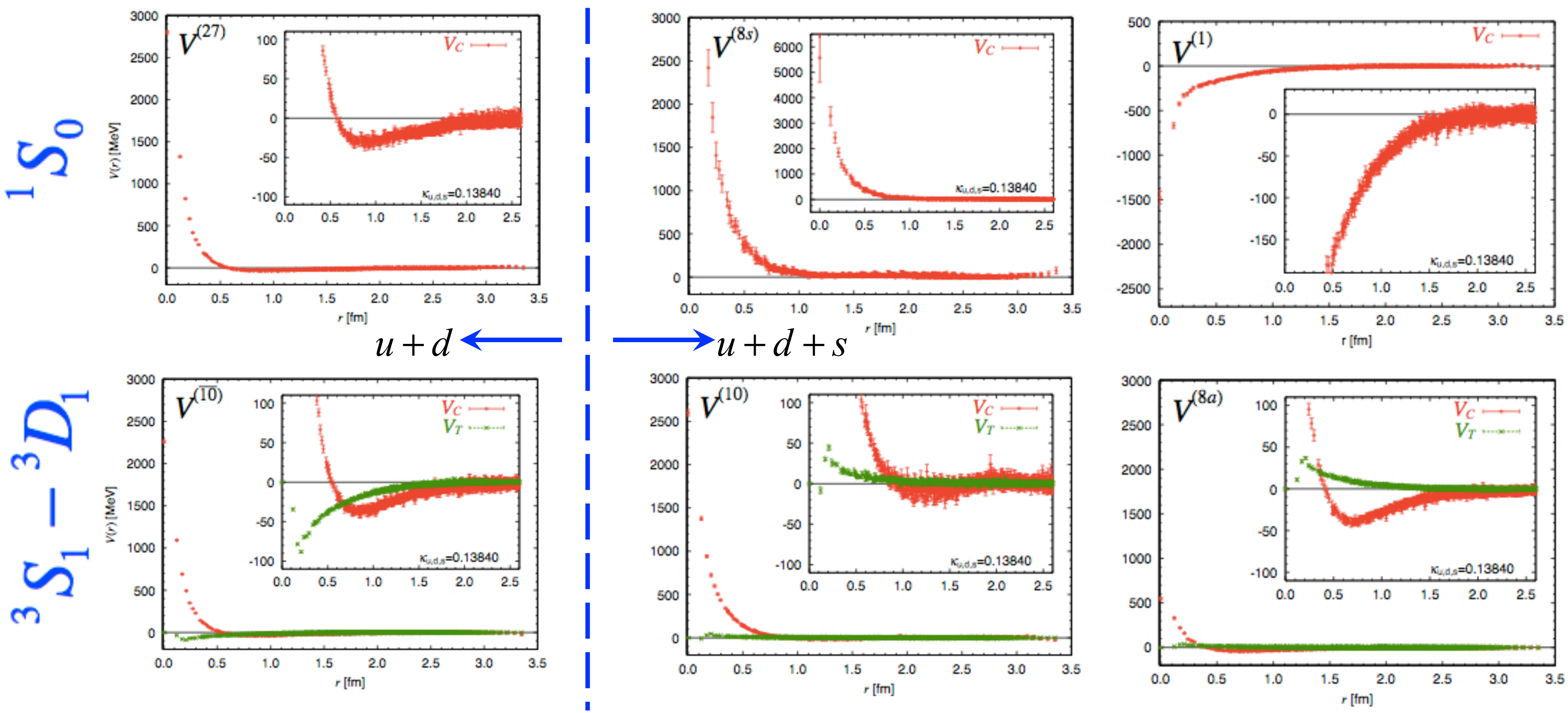

◆ Strong flavor dependence

◆ Short distance behaviors are consistent with quark Pauli blocking picture.

Hyperon Forces

[T.Inoue et al., PRL106(2011)162002.] (37)

◆ Bound H-dibaryon in flavor SU(3) limit

Entirely attractive potential

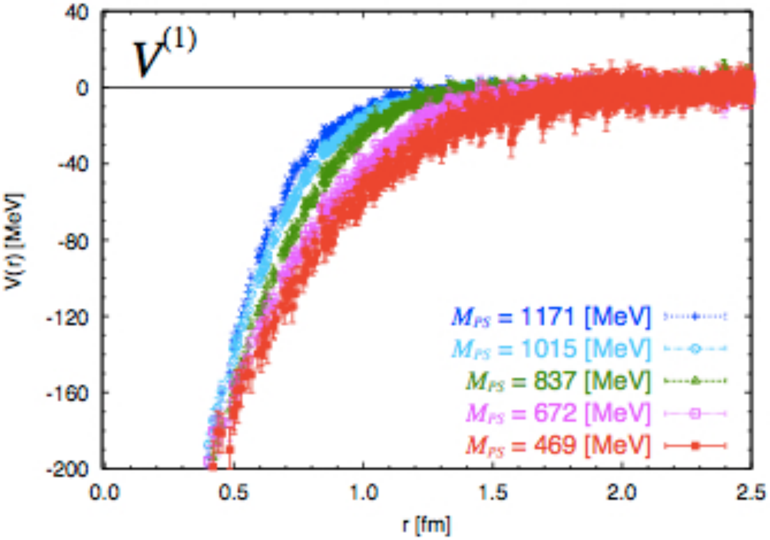

Bound H-dibaryon

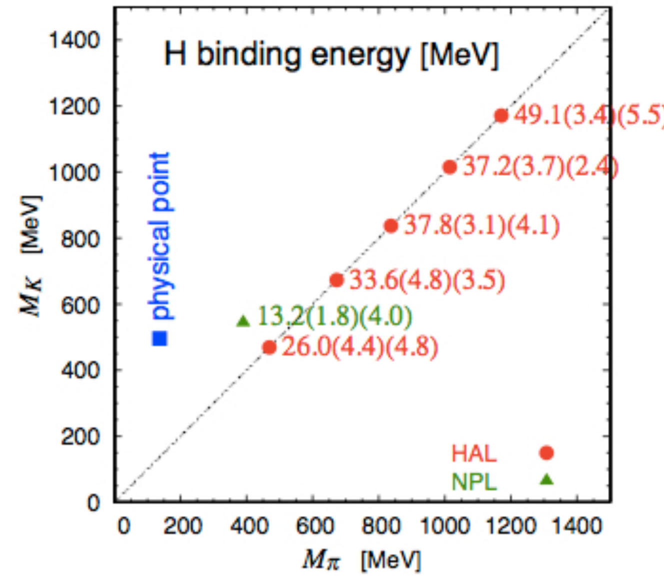

◆ Flavor SU(3) breaking for real world.

➔ BB threshold splits into ΛΛ, NΞ, ΣΣ thresholds

➔ Coupled channel system of

$$\Lambda\Lambda - N\Xi - \Sigma\Sigma$$

SU(3) lat ➔ **Physical point**

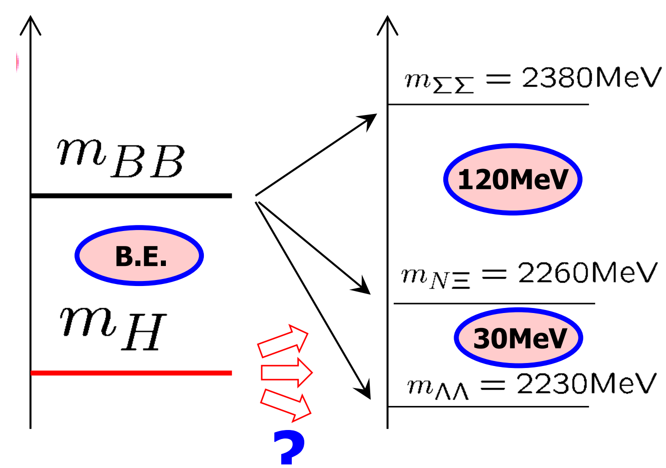

Hyperon Forces

◆Coupled ch. in finite volume:

- In finite volume,
  it is not easy to impose incoming B.C.'s separately.

$$|n,in\rangle = |N\Lambda,in\rangle, |N\Sigma,in\rangle$$

➔ **Coupled ch. extension** of **the finite vol. method** is **NOT straightforward**.

[S.He, et al., JHEP07(2005)011]

- Many solutions are proposed.
  - M.Lage, et al., PLB681
  - V.Bernard et al., PLB681
  - A.M.Torres, et al., PRD85
  - M.Doring et al., JHEP1201
  - M.T.Hansen et al., PRD86
  - R.A.Briceno et al., PRD88
  - M.Doring et al., EPJA48
  - N.Li et al., PRD87
  - P.Guo et al., PRD88
  - J.-J.Wu et al., PRC90.
  - S.Aoki et al., PJAB87

Hyperon Forces

[S.Aoki et al., Proc.Japan Acad.B87(2011)509.]

◆ **Coupled ch. extension** of **HAL QCD method** is **straightforward.**

$$\Psi_n(\vec{x}-\vec{y}) \equiv \begin{bmatrix} \langle 0 | N(\vec{x})\Lambda(\vec{y}) | n, in \rangle \\ \langle 0 | N(\vec{x})\Sigma(\vec{y}) | n, in \rangle \end{bmatrix}$$

$$\begin{cases} E \equiv \sqrt{m_N^2 + \vec{p}_{N\Lambda}^{\,2}} + \sqrt{m_\Lambda^2 + \vec{p}_{N\Lambda}^{\,2}} \\ \quad = \sqrt{m_N^2 + \vec{p}_{N\Sigma}^{\,2}} + \sqrt{m_\Sigma^2 + \vec{p}_{N\Sigma}^{\,2}} \end{cases}$$

"Coupled channel Schrodinger eq."

$$\begin{bmatrix} \left(\frac{\vec{p}_{N\Lambda}^{\,2}}{2\mu_{N\Lambda}} + \frac{\Delta}{2\mu_{N\Lambda}} \right) \psi_{N\Lambda}(\vec{r};n) \\ \left(\frac{\vec{p}_{N\Sigma}^{\,2}}{2\mu_{N\Sigma}} + \frac{\Delta}{2\mu_{N\Sigma}} \right) \psi_{N\Sigma}(\vec{r};n) \end{bmatrix} = \int d^3r' \begin{bmatrix} U_{N\Lambda;N\Lambda}(\vec{r},\vec{r}\,') & U_{N\Lambda;N\Sigma}(\vec{r},\vec{r}\,') \\ U_{N\Sigma;N\Lambda}(\vec{r},\vec{r}\,') & U_{N\Sigma;N\Sigma}(\vec{r},\vec{r}\,') \end{bmatrix} \cdot \begin{bmatrix} \psi_{N\Lambda}(\vec{r}\,';n) \\ \psi_{N\Sigma}(\vec{r}\,';n) \end{bmatrix}$$

- ☐ U(r,r') is state-independent, i.e.,
  It works for any linear comb's |n,in> = |NΛ,in>α+ |NΣ,in>β.
  ➔ Extract U(r,r') in the **finite** vol.

- ☐ Use U(r,r') in the **inifinite** vol.
  to obtain the NBS wave funcs. of these states separately. ➔ **S-matri**x.

- ☐ Again, the single state saturation is not needed for HAL QCD potential.

Hyperon Forces

[K.Sasaki@EMMI workshop(CERN)]

ΛΛ, NΞ, ΣΣ (I=0) $^1S_0$ channel

Esb1 : mπ= 701 MeV
Esb2 : mπ= 570 MeV
Esb3 : mπ= 411 MeV

Diagonal elements

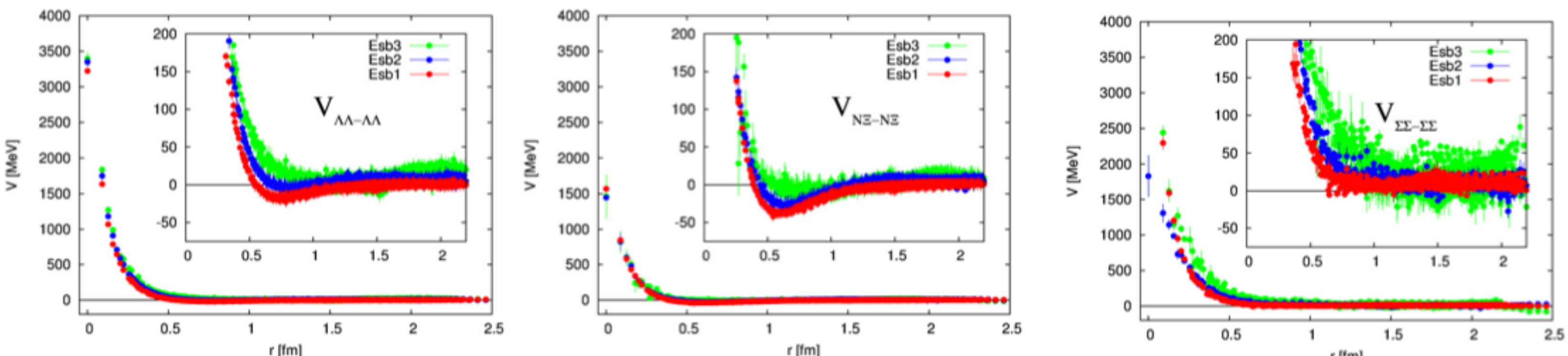

shallow attractive pocket | Deeper attractive pocket | Strongly repulsive

All channels have repulsive core

Off-diagonal elements

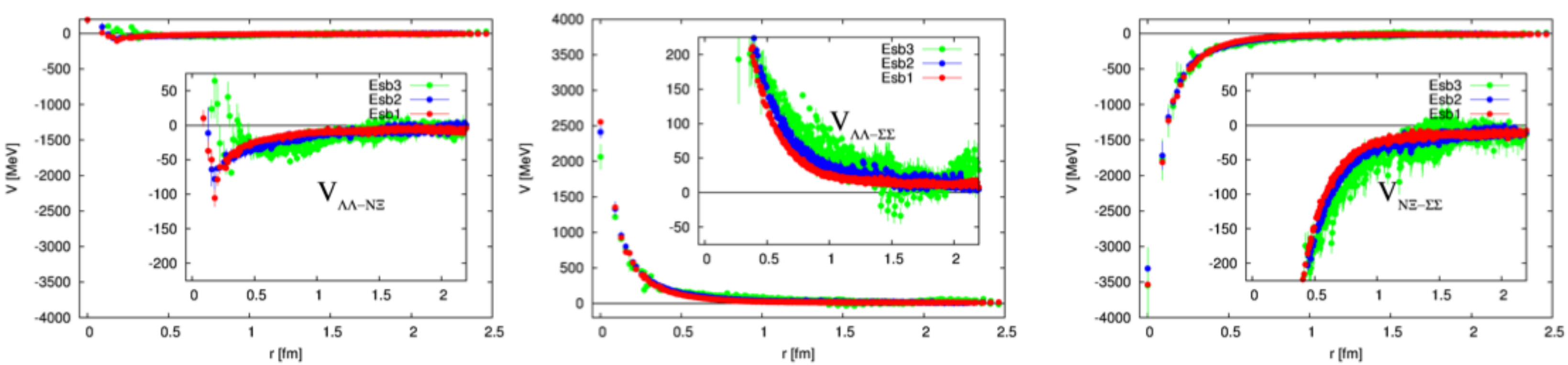

In this channel, our group found the "H-dibaryon" in the SU(3) limit.

Hyperon Forces

[K.Sasaki@EMMI workshop(CERN)]

$\Lambda\Lambda$ and $N\Xi$ phase shifts

- N_f = 2+1 full QCD with L = 2.9fm

Preliminary!

m_π = 700 MeV | m_π = 570 MeV | m_π = 410 MeV

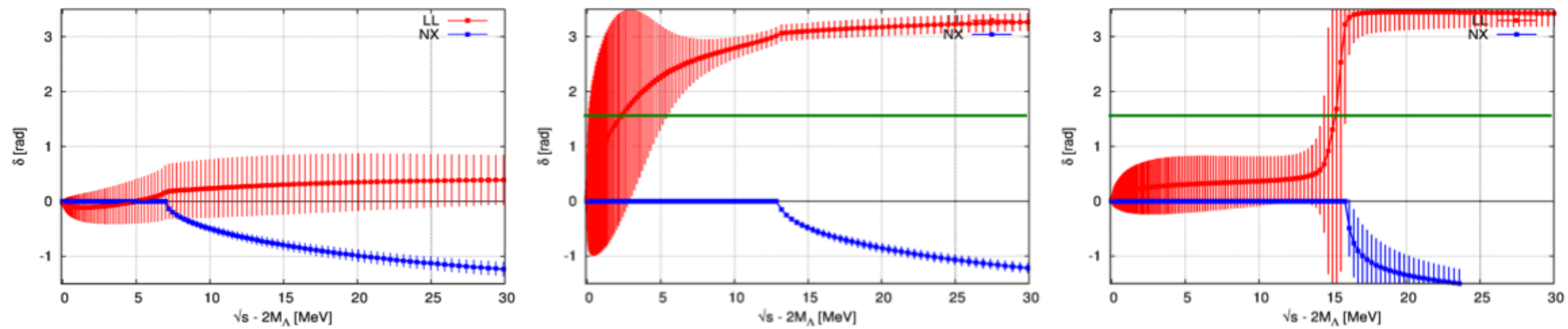

- m_π = 700 MeV : bound state
- m_π = 570 MeV : resonance near $\Lambda\Lambda$ threshold
- m_π = 410 MeV : resonance near $N\Xi$ threshold

H-dibaryon is unlikely bound state

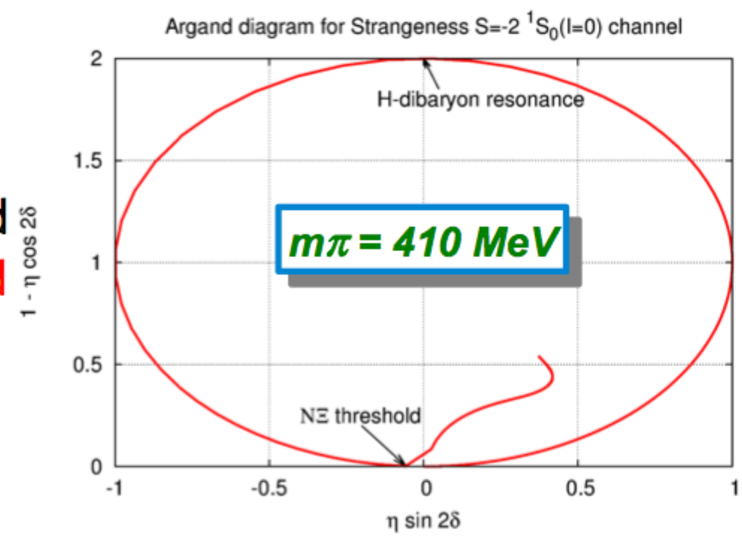

Hyperon Forces

◆ ΛN forces up to NLO

$$V_{\Lambda N} = V_{\mathrm{C;S=0}}(r)\mathbb{P}^{(S=0)} + V_{\mathrm{C;S=1}}(r)\mathbb{P}^{(S=1)} + V_{\mathrm{T}}(r)\left(3(\hat{r}\cdot\vec{\sigma}_\Lambda)(\hat{r}\cdot\vec{\sigma}_N) - \vec{\sigma}_\Lambda\cdot\vec{\sigma}_N\right)$$

$$+V_{\mathrm{LS}}(r)\vec{L}\cdot(\vec{s}_\Lambda + \vec{s}_N) + \underbrace{V_{\mathrm{ALS}}(r)\vec{L}\cdot(\vec{s}_\Lambda - \vec{s}_N)}_{\text{NEW TERM: Anti-symmetric LS}} + O(\nabla^2)$$

◆ Spin-orbit puzzle in ΛN sector

Conventional Nuclei

Large Spin-Orbit Splitting

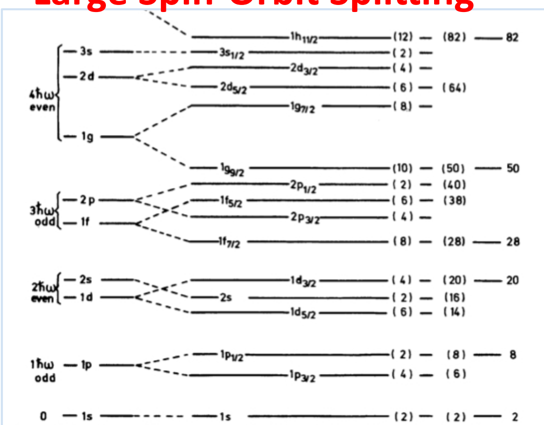

Figure 2.5. Schematic nuclear levels of the shell model with spin orbit term.

Λ Hyper Nuclei

Small Spin-Orbit Splitting for Λ

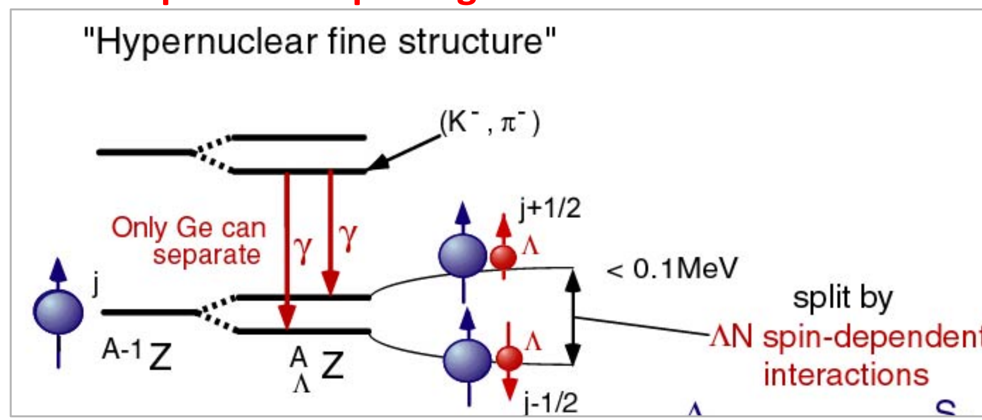

◆ Λ-spin dependent Spin-orbit force

$$V_{\mathrm{LS}}^{(\Lambda)}(r) \equiv V_{\mathrm{LS}}(r) + V_{\mathrm{ALS}}(r) \sim 0$$ ➔ LS-ALS cancellation

✧ Quark model ➔ Strong cancellation

✧ Meson exch. Model ➔ Weak cancellation

Hyperon Forces

[N.Ishii@Lattice 2013]

◆ **Parity-odd** hyperon potentials in the **flavor SU(3) limit**.

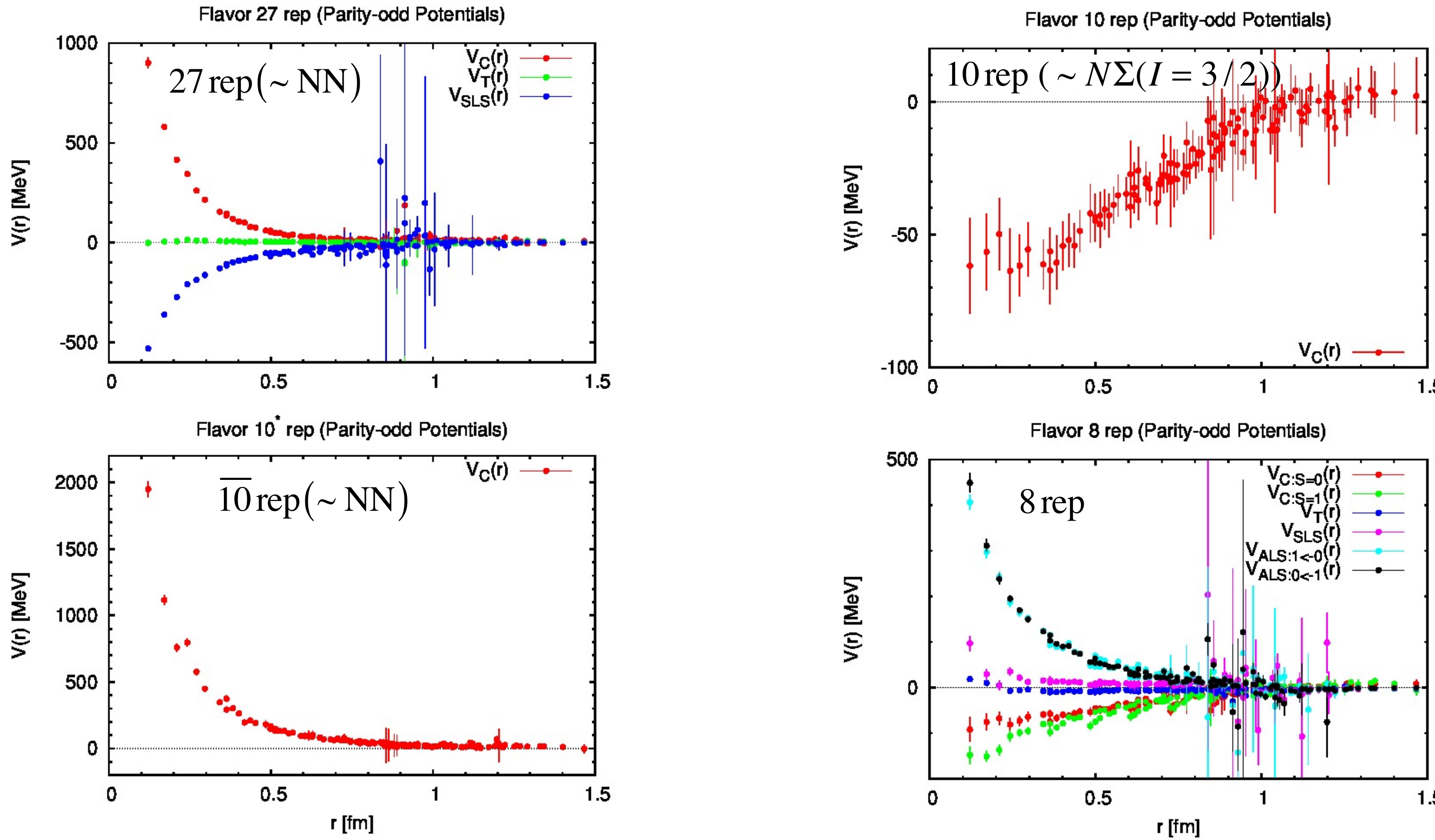

◆ Repulsive core for irreps. 27 and 10^*（∼NN）. No repulsive core for irreps. 10 and 8.

(These are consistent with quark model)

◆ Strong LS for irrep. 27 (∼NN). Weak LS for irrep. 8.

◆ Strong anti-symmetric LS (irrep. 8).

Hyperon Forces

◆ΛN-ΣN coupled channel potentials (odd parity sector)

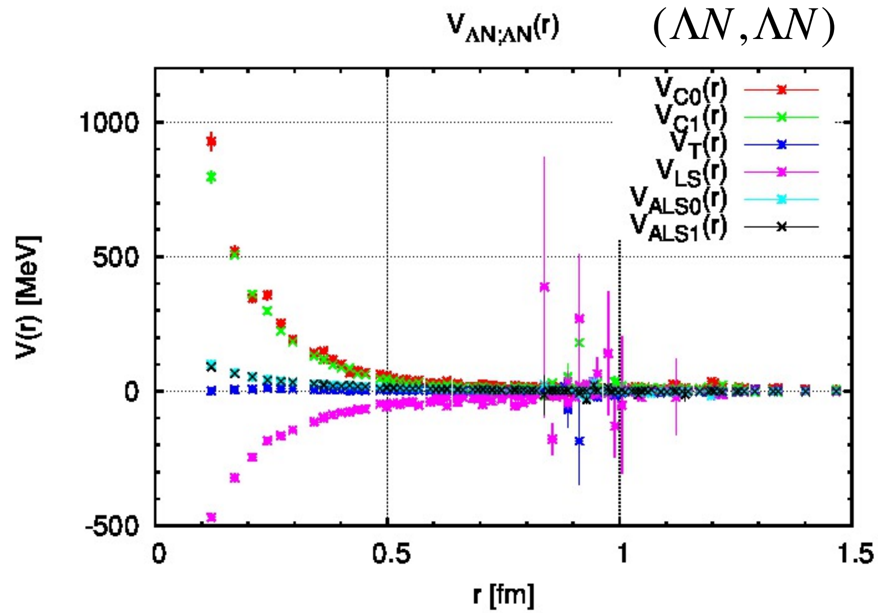

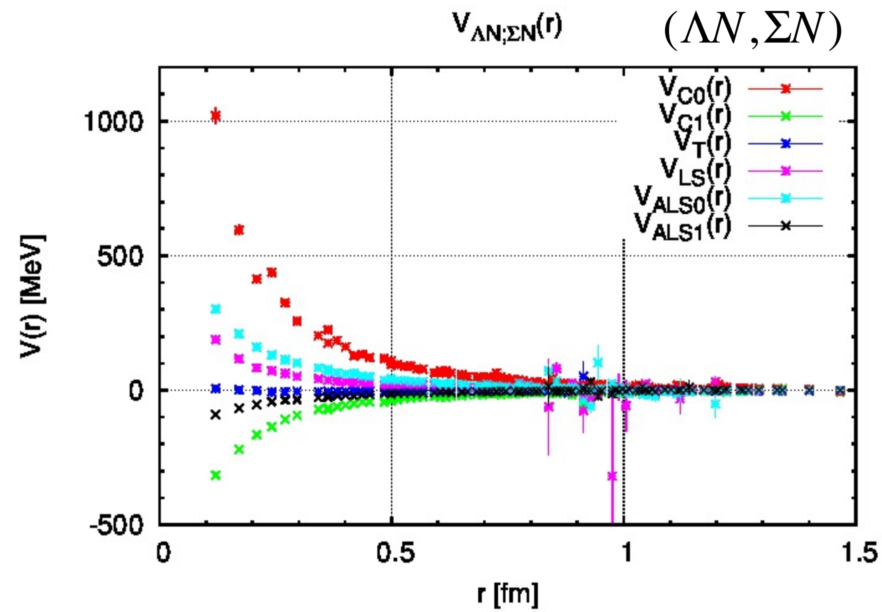

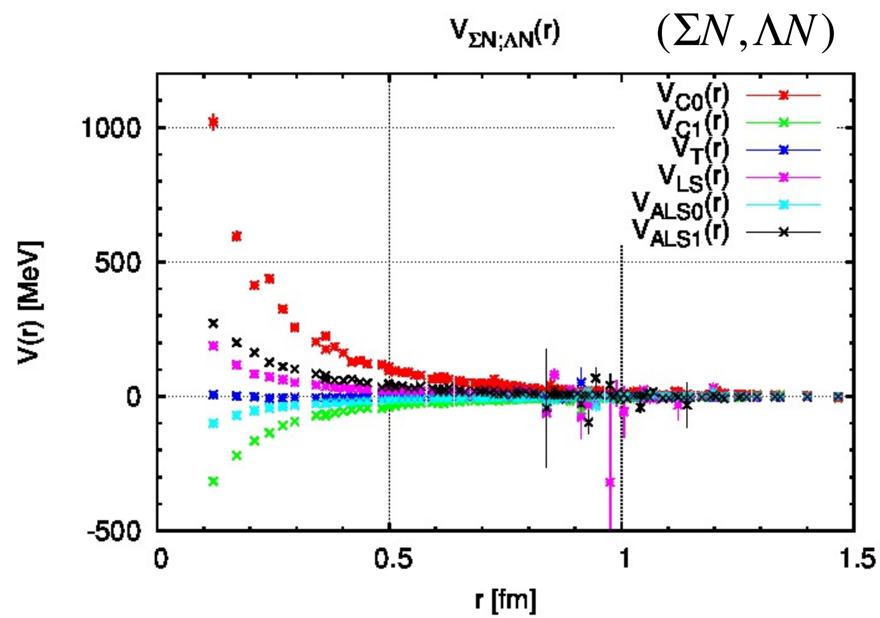

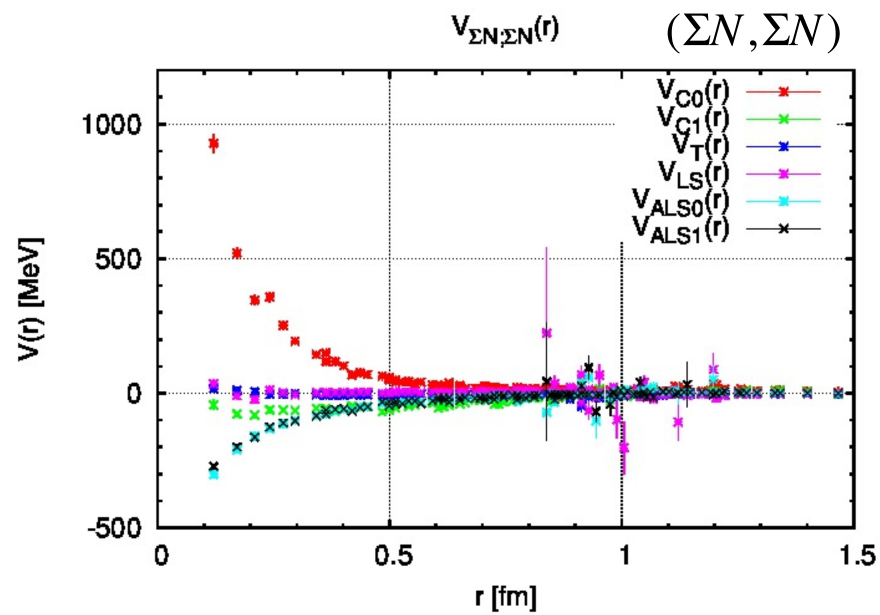

Hyperon Forces

[N.Ishii et al. coming soon]

① ΛN sector of ΛN-ΣN coupled ch. potential (parity-odd sector)

$V_{\Lambda N;\Lambda N}(r)$

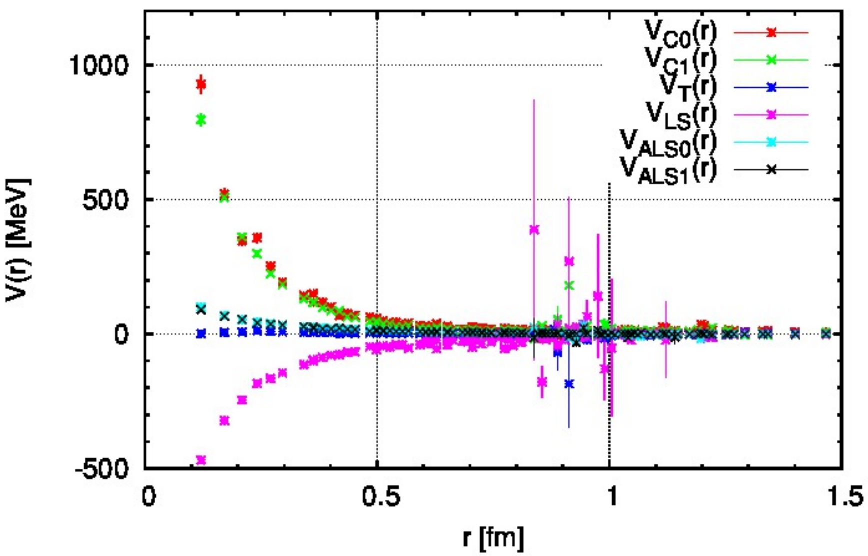

② effective ΛN potential after ΣN ch. is integrated out.

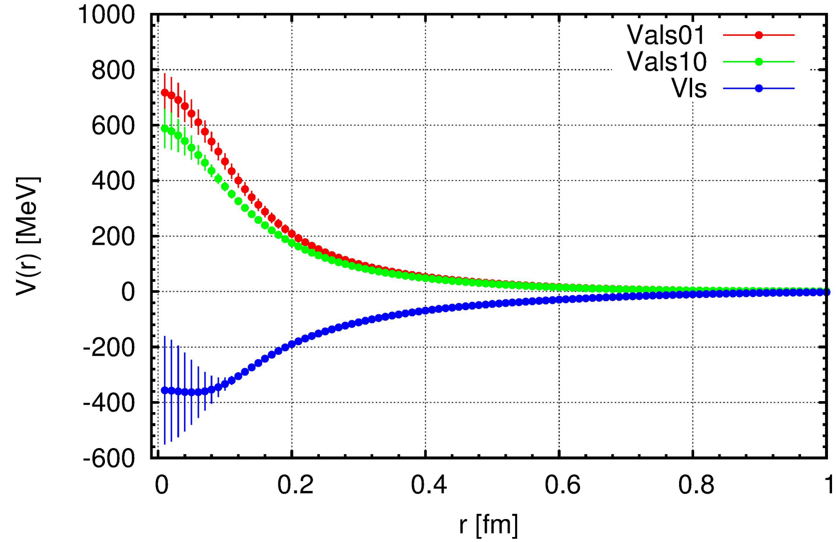

$$V_{\Lambda N;\Lambda N} = \left(\frac{1}{2}V_{\mathrm{C}}^{(\overline{10})} + \frac{1}{2}V_{\mathrm{C;S=0}}^{(8)}\right)\mathbb{P}^{(S=0)} + \left(\frac{1}{10}V_{\mathrm{C:S=1}}^{(8)} + \frac{9}{10}V_{\mathrm{C}}^{(27)}\right)\mathbb{P}^{(S=1)}$$

$$+\left(\frac{1}{10}V_{\mathrm{T}}^{(8)} + \frac{9}{10}V_{\mathrm{T}}^{(27)}\right)\left(3(\hat{r}\cdot\vec{\sigma}_\Lambda)(\hat{r}\cdot\vec{\sigma}_N) - \vec{\sigma}_\Lambda\cdot\vec{\sigma}_N\right)$$

$$+\left(\frac{1}{10}V_{\mathrm{LS}}^{(8)} + \frac{9}{10}V_{\mathrm{LS}}^{(27)}\right)\vec{L}\cdot(\vec{s}_\Lambda + \vec{s}_N)$$

$$+\left(\frac{1}{2\sqrt{5}}V_{\mathrm{ALS}}^{(8)}\right)\cdot\vec{L}\cdot(\vec{s}_\Lambda - \vec{s}_N)$$

included

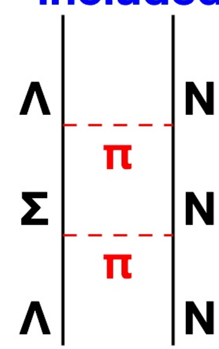

ΛN-ΣN coupling is important

Baryon-baryon potentials at “physical point”

$$m_\pi = 145\,\mathrm{MeV}$$

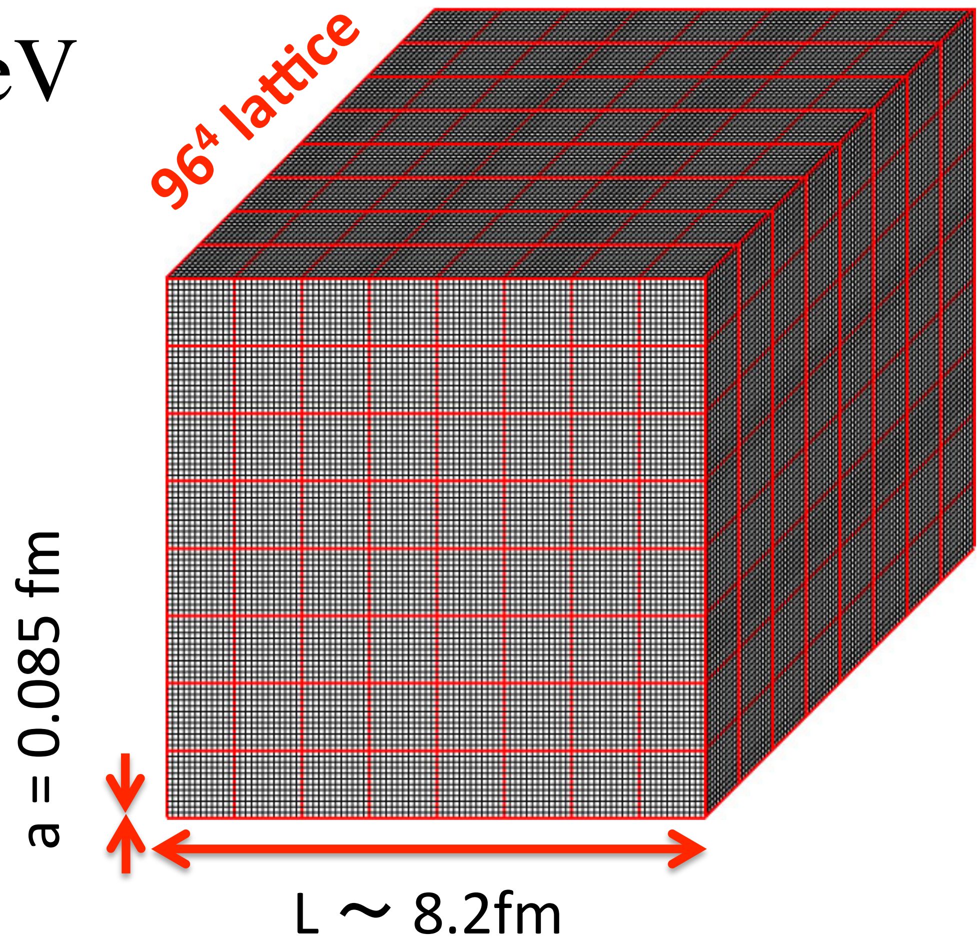

Baryon-baryon potentials at "physical point"

[T.Doi, Session 4a]

S=0 sector

(20*4 src pt. used)

NN-Potentials

$^1S_0$

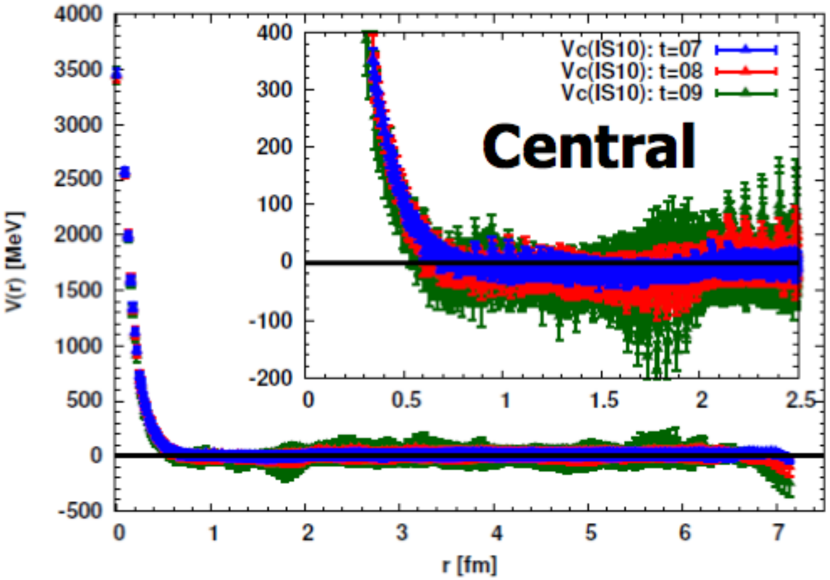

$^3S_1$-$^3D_1$

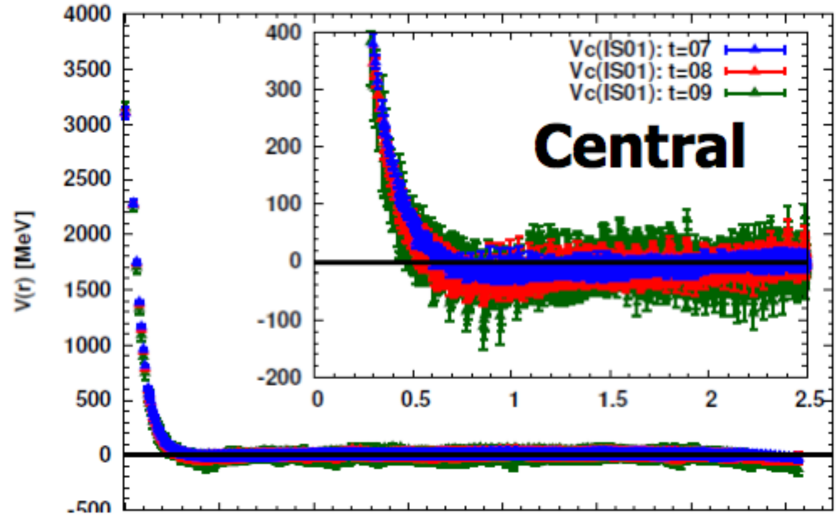

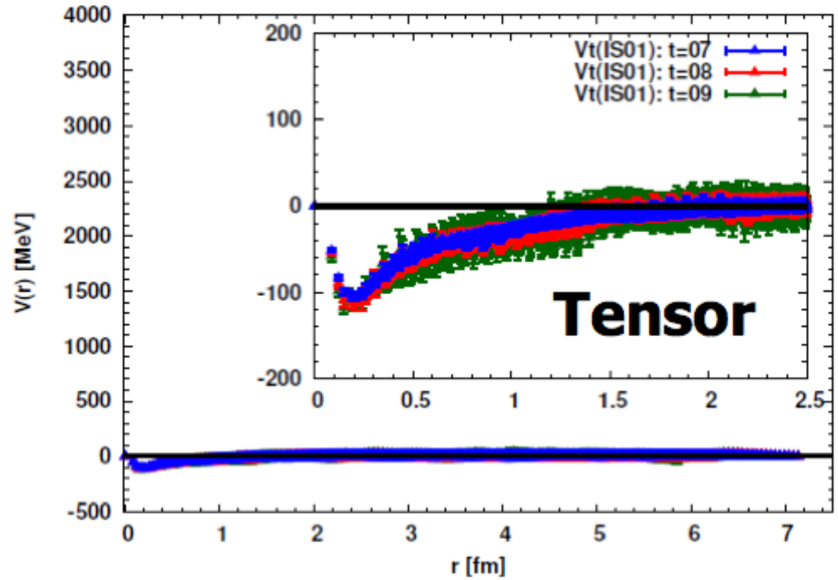

Preliminary

- **Vc: repulsive core**
  + long-range attraction (?)
- **Vt: tensor force clearly visible**

Baryon-baryon potentials at "physical point"

[T.Doi, Session 4a]

S=-4 sector

(20*4 src pt. used)

ΞΞ-Potentials

$^1S_0$

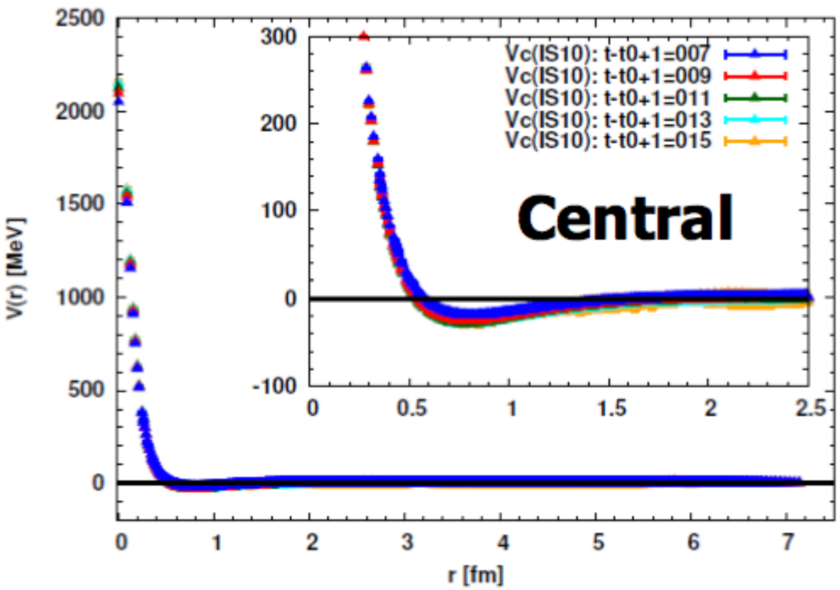

$^3S_1$-$^3D_1$

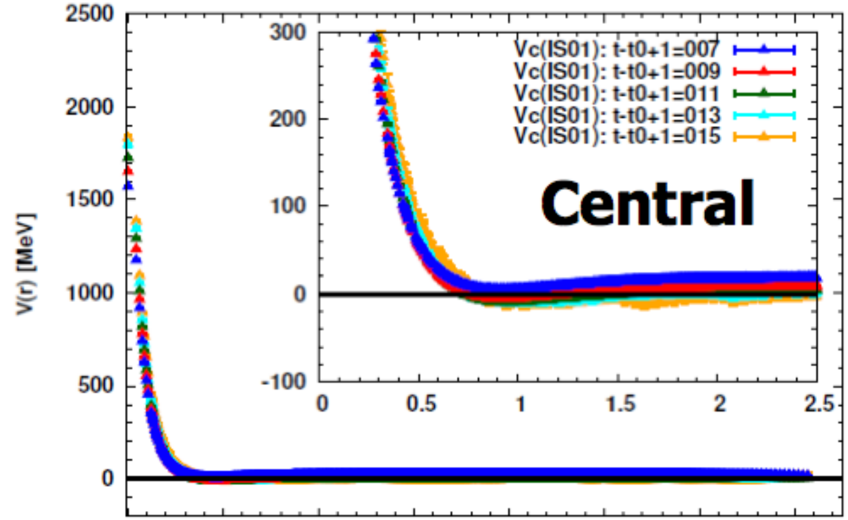

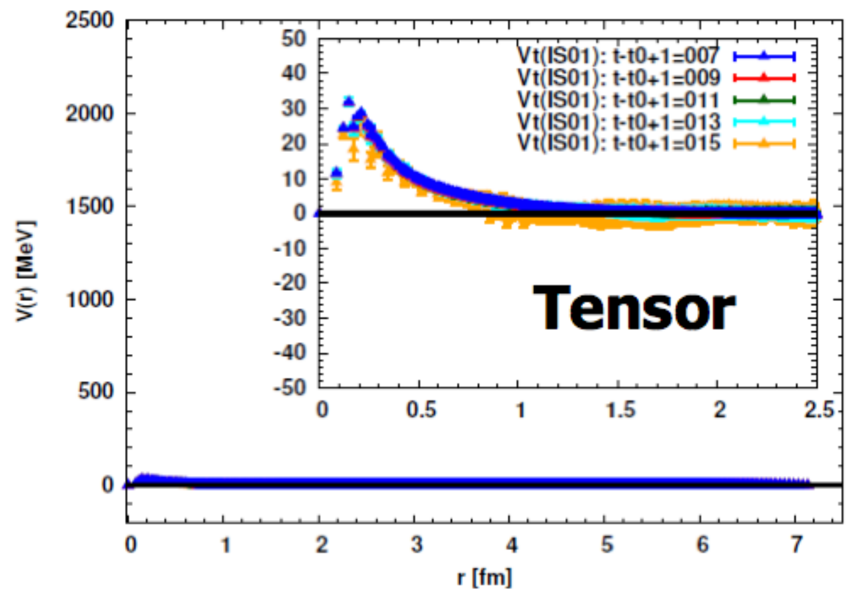

Preliminary

- $^1S_0$ ~ 27-plet
  ⇔ NN($^1S_0$) + SU(3) breaking
- $^3S_1$-$^3D_1$ ~ 10-plet
  ⇔ unique w/ hyperon DoF

Baryon-baryon potentials at “physical point”

[H.Nemura, Session 4a]

Very preliminary result of LN potential at the physical point

S=-1 sector

(8*4 src pt. used)

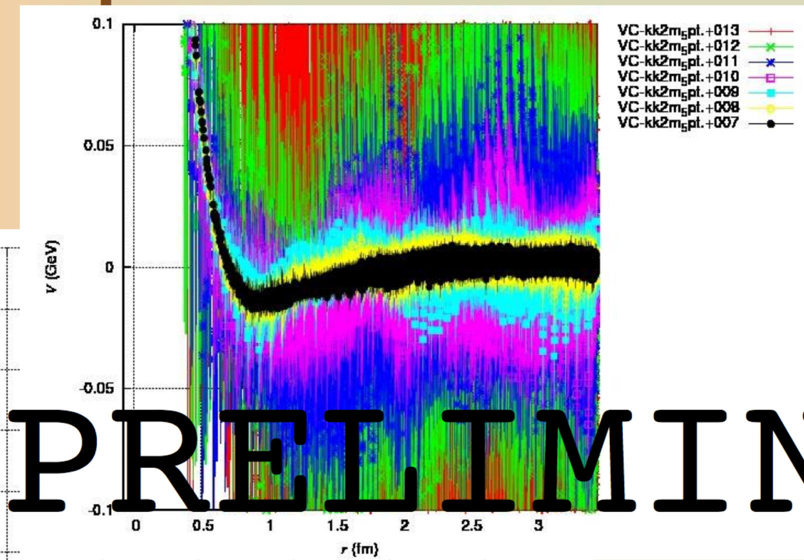

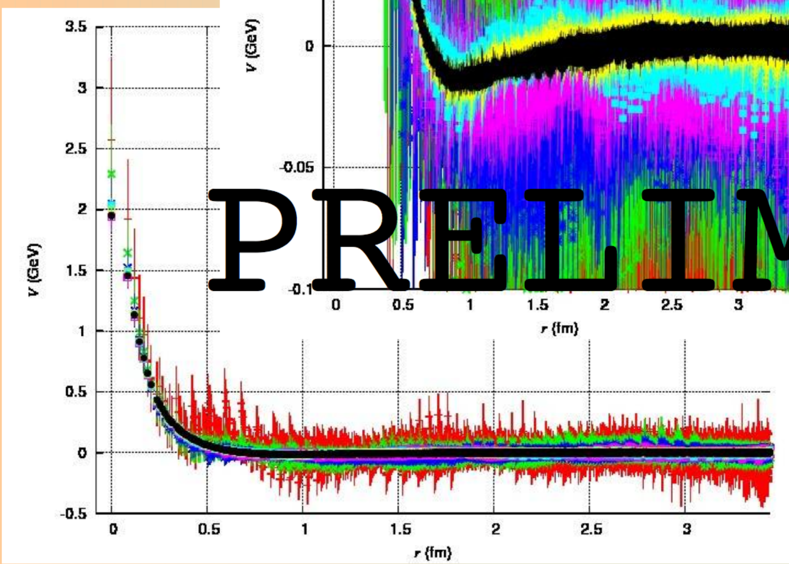

PRELIMINARY

$V_C({}^3E_1)$

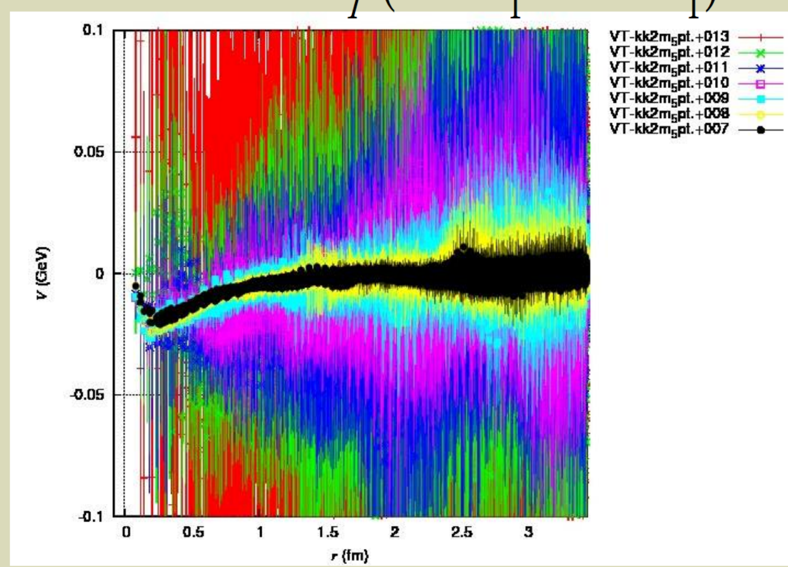

$V_T({}^3S_1 - {}^3D_1)$

#stat: (this/planned) < 0.1

Baryon-baryon potentials at "physical point"

[K.Sasaki, Session 4a]

S=-2 sector

$\Lambda\Lambda$, $N\Xi$, $\Sigma\Sigma$ (I=0) $^1S_0$ channel near the physical point

(16*4 src pt. used)

- N_f = 2+1 full QCD with L = 8fm, m_π = 145 MeV

Preliminary!

Diagonal elements

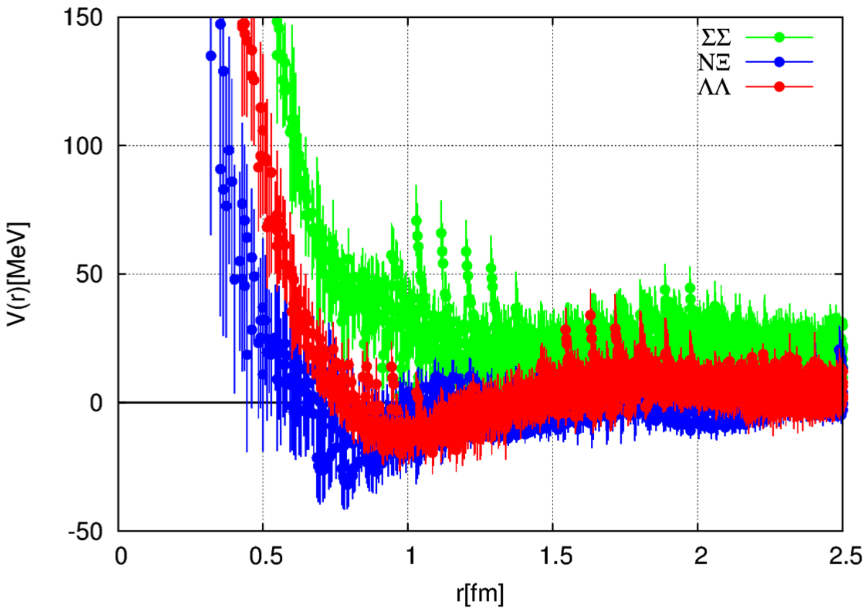

Off-diagonal elements

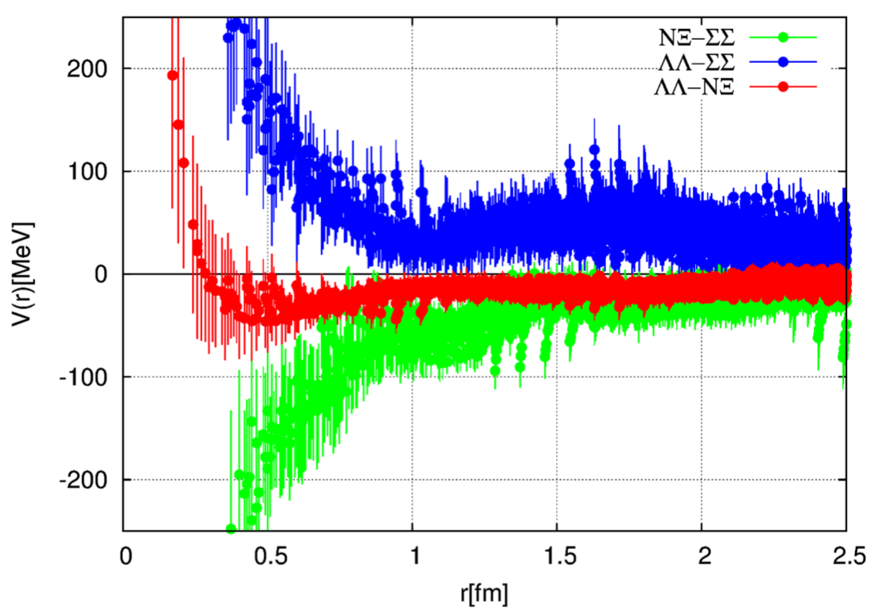

- All diagonal element have a repulsive core $\Sigma\Sigma$–$\Sigma\Sigma$ potential is strongly repulsive.
- Off-diagonal potentials are relatively strong except for $\Lambda\Lambda$–$N\Xi$ transition
- We need more statistics to discuss physical observables through this potential.

Baryon-baryon potentials at “physical point”

ΛΛ and NΞ (I=0) $^1S_0$ phase shift (2ch calculation)

▶ N_f = 2+1 full QCD with L = 8fm, ***mπ = 145 MeV***

Preliminary!

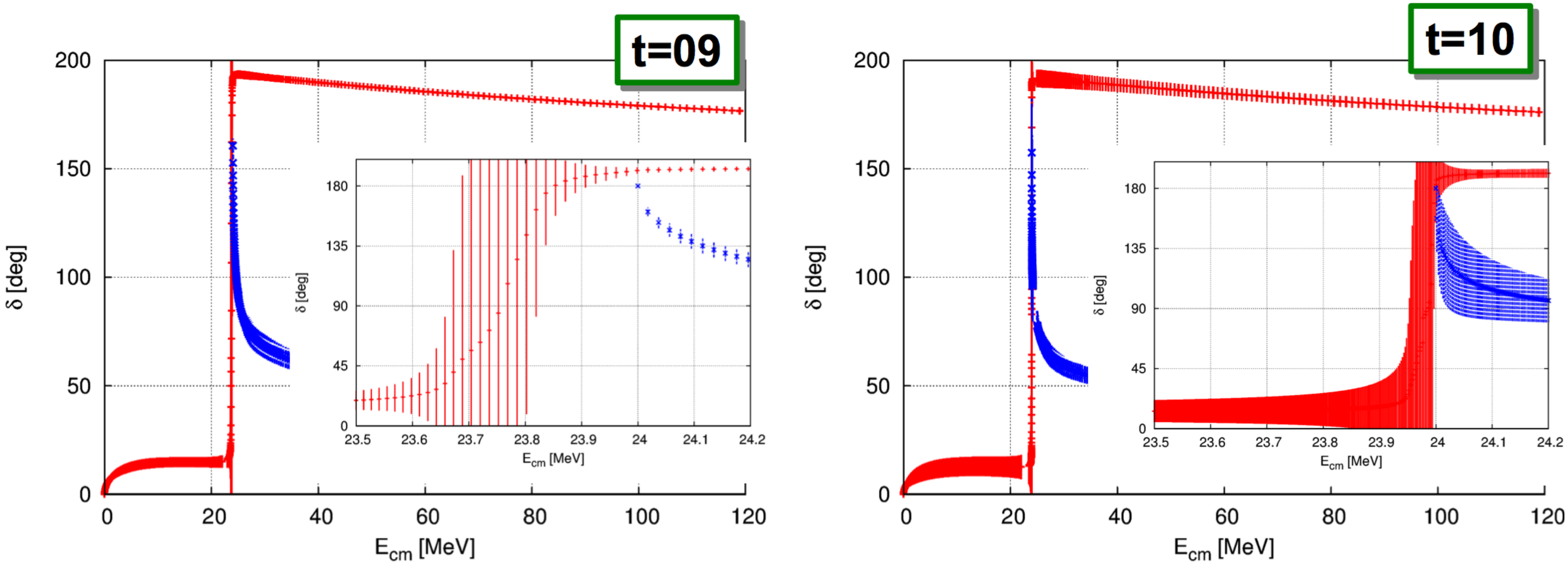

- ΛΛ and NΞ phase shift is calculated by using 2ch effective potential.
- For both cases, we found the sharp resonance just below the NΞ threshold.
- Time slice saturation should be checked.
- 3ch calculation(need more statistics)

Summary

Summary

◆Determination of BB potentials at "physical point" LQCD.

(m_{pion}=145 MeV, L〜8.2 fm, 96^4 lattice, a〜0.085fm)

- ❖ Currently ongoing. (Number of src. points: 4*20 ➔ 4*96)
- ❖ We have presented some of the preliminary results.

◆Potential method v.s. direct method

- ❖ These two are consistent.
- ❖ **We have to be very careful against the ground state saturation.**
  Many cancellations are involved, which can lead to fake plateaux.
- ❖ For direct method with smear src., systematic uncertainty appear to be large.
  Results should be checked by other method / other source.
  This applies to the results of (i) Yamazaki group (ii) NPL QCD

◆LQCD calculation of BB potentials (General Aspects)

- ❖ Potentials faithful to the scattering observable.
- ❖ **Special strategy** against the problem of **the ground state saturation**:
  The potenital method does not need ground state saturation.
- ❖ Wide range of application
  NN, NY, YY, NNN, negative parity, LS and anti-symmetric LS potential, etc.
  [Results involving decuplet baryons ➔ K.Sasaki@MPMBI2015[Sept.12(Sat)]]

Backup Slides

HALQCD method

SKIP

◆Proof of existence of E-indep. U(r,r’)

◆Assumption:

Linear indep. of NBS wave func’s for E < Eth.

➔ Dual basis exists

$$\int d^3r\,\tilde{\psi}_{\vec{k}'}(\vec{r})\psi_{\vec{k}}(\vec{r}) = (2\pi)^3\delta^3(\vec{k}'-\vec{k})$$

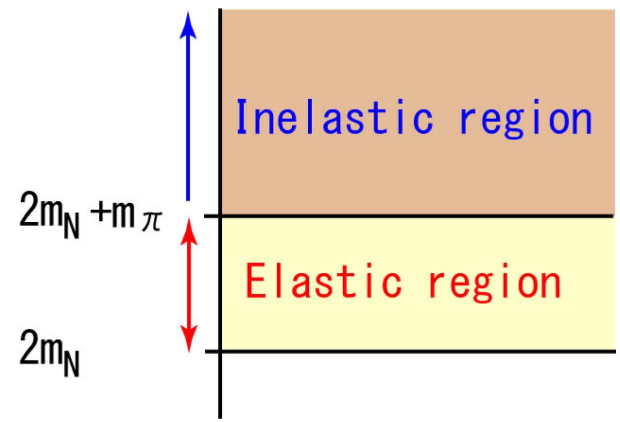

◆Proof:

$$K_{\vec{k}}(\vec{r}) \equiv \left(k^2/m_N - H_0\right)\psi_{\vec{k}}(\vec{r})$$

$$K_{\vec{k}}(\vec{r}) = \int \frac{d^3k'}{(2\pi)^3} K_{\vec{k}'}(\vec{r}) \int d^3r'\,\tilde{\psi}_{\vec{k}'}(\vec{r})\psi_{\vec{k}}(\vec{r})$$

$$= \int d^3r' \left\{ \int \frac{d^3k}{(2\pi)^3} K_{\vec{k}'}(\vec{r})\tilde{\psi}_{\vec{k}'}(\vec{r}') \right\} \psi_{\vec{k}}(\vec{r}')$$

$$\left(k^2/m_N - H_0\right)\psi_{\vec{k}}(\vec{r}) = \int d^3r'\,U(\vec{r},\vec{r}')\psi_{\vec{k}}(\vec{r}')$$

$$U(\vec{r},\vec{r}') \equiv \int \frac{d^3k'}{(2\pi)^3} K_{\vec{k}'}(\vec{r})\tilde{\psi}_{\vec{k}'}(\vec{r})$$

U(r,r’) does not depend on E
because of the integration of k’.

Nuclear Force from Lattice QCD

Volume dependence of the potential.

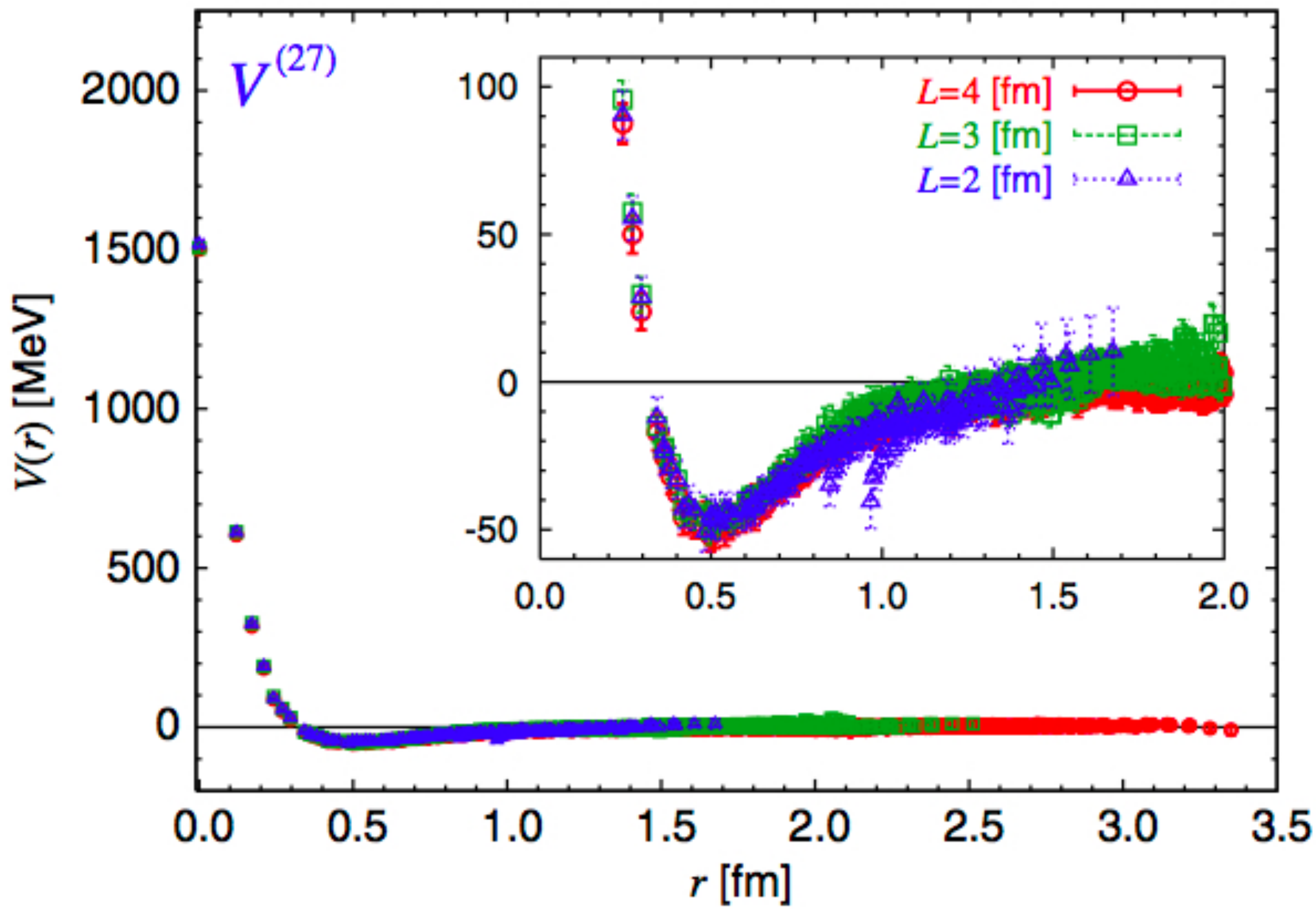

Nuclear Forces

[Inoue et al.,NPA881(2012)28] (57)

Similar behavior is seen in NF=3 calculation (flavor SU(3) limit)

- m_{PS}=672-1171 MeV: attraction shrinks as decreasing quark mass.
- m_{PS}=**469**-672 MeV: **turning point**: attraction starts to increase.
- m_{PS}=0 -**469** MeV: attraction increase (← Our expectation !)

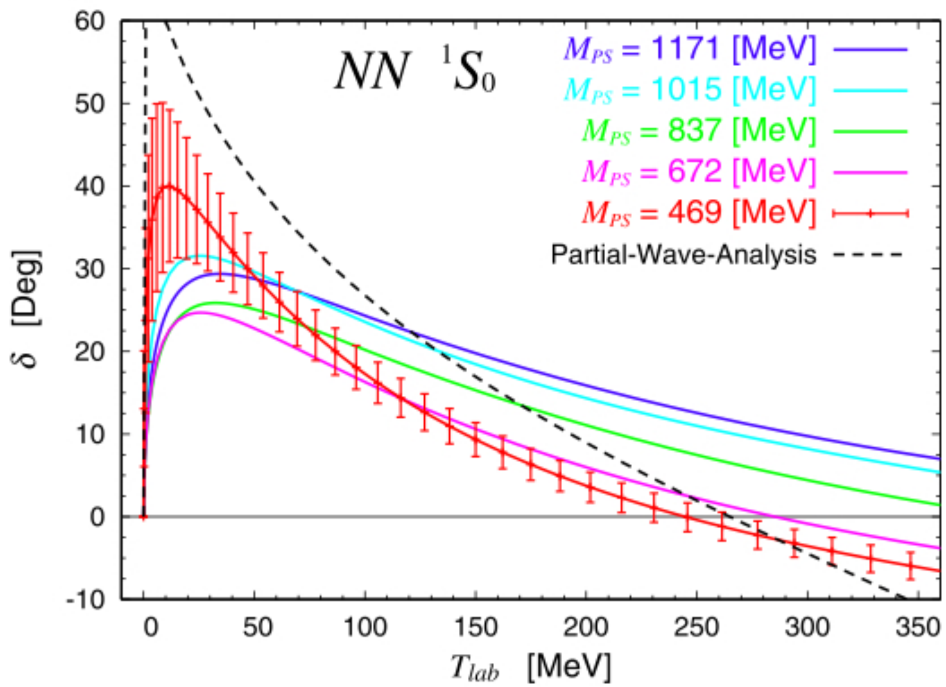

- For the similar thing to happen for NF=2+1,pion mass has to be smaller. Nuclear force for NF=3 is generally more attractive than NF=2+1.

$$\#(\text{Goldstone mode}) = \begin{cases} 3 & (N_F = 2+1) \\ 8 & (N_F = 3) \end{cases}$$

Nuclear Forces

SKIP

◆Momentum wall source

$$\overline{\mathcal{J}}_{\alpha\beta}(\vec{p}) \equiv \sum_{\vec{x}_1,\cdots,\vec{x}_6} \overline{p}_\alpha(\vec{x}_1,\vec{x}_2,\vec{x}_3)\overline{n}_\beta(\vec{x}_4,\vec{x}_5,\vec{x}_6)\cdot\exp\left(i\,\vec{p}\cdot(\vec{x}_3-\vec{x}_6)\right)$$

$$\begin{cases} p_\alpha(x_1,x_2,x_3) \equiv \epsilon_{abc}\left(u_a(x_1)C\gamma_5 d_b(x_2)\right)u_{c;\alpha}(x_3) \\ n_\beta(x_4,x_5,x_6) \equiv \epsilon_{abc}\left(u_a(x_4)C\gamma_5 d_b(x_5)\right)d_{c;\beta}(x_6) \end{cases}$$

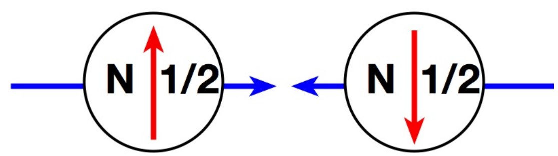

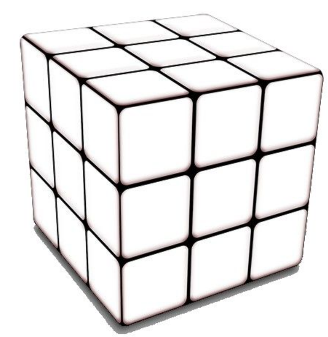

◆Cubic group irrep. theory to access p-wave sector

$$\overline{\mathcal{J}}_{\alpha\beta}(|\,\vec{p}\,|) \equiv \frac{1}{48}\sum_{g\in O_h}\chi^{(\Gamma)}(g^{-1})\cdot\overline{\mathcal{J}}_{\alpha'\beta'}(g\cdot\vec{p})S_{\alpha'\alpha}(g^{-1})S_{\beta'\beta}(g^{-1})$$

[K.Murano et al., PLB735(2014)19.]

HAL QCD method: Determination of potentials

We have a special strategy for the ground state saturation.

◆ Def. R-correlator

[Ishii et al.,PLB712(2012)437]

$$R(\vec{x}-\vec{y},t) \equiv e^{2mt} \left\langle 0 \middle| T\left[B(\vec{x},t)B(\vec{y},t)\cdot \overline{BB}(t=0)\right] \middle| 0 \right\rangle$$

$$= \sum_n \psi_{k_n}(\vec{x}-\vec{y})\cdot \exp\left(-(E_n-2m)t\right)\cdot a_n$$

$$\psi_{k_n}(\vec{x}-\vec{y}) \equiv \left\langle 0 \middle| B(\vec{x})B(\vec{y}) \middle| n \right\rangle$$

◆ Two-particle energy in CM frame satisfies

$$E \equiv 2\sqrt{m^2+k^2} \quad \Rightarrow \quad \frac{k^2}{m} = \frac{1}{4m}(E-2m)^2 + (E-2m)$$

◆ HAL QCD potential satisfies Schroedinger eq.

$$\left(-H_0 + k_n^2/m\right)\psi_{k_n}(\vec{r}) = \int d^3r' V(\vec{r},\vec{r}')\, \psi_{k_n}(\vec{r}')$$

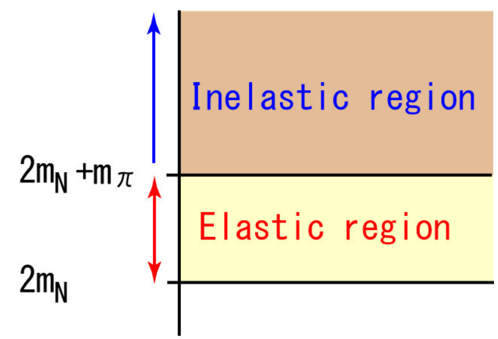

◆ R-corr. satisfies **time-dependent Schroedinger-like eq.**

$$\boxed{\left(-H_0 + \frac{1}{4m}\frac{\partial^2}{\partial t^2} - \frac{\partial}{\partial t}\right) R(\vec{r},t) = \int d^3r' V(\vec{r},\vec{r}') R(\vec{r}',t)}$$

- ☐ Only **Elastic saturation** is needed.(**Ground state saturation is not needed.**)
- ☐ **Elastic saturation** is much easier than **single state saturation**.